Electronic supplementary materials *Mendeleev Commun.*, 2024, **34**, 113–115

Quaternary phosphonium salts based on quinopimaric acid

Anastasiya M. Shinkareva, Andrey V. Nemtarev, Denis V. Chachkov, Alexei B. Dobrynin, Igor A. Litvinov and Vladimir F. Mironov

Table of Contents

Experimental Section

General remarks. The NMR spectra were recorded at 25 °C using a Bruker Avance-400 NMR spectrometer (400.0 MHz, ^{1}H; 100.6 MHz, ^{13}C; 162 MHz, ^{31}P), BrukerAvance-500 (125.8 MHz, ^{13}C) or BrukerAvance-600 (600 MHz, ^{1}H). Chemical shifts are referenced to the residual solvent peak and reported in ppm (δ scale) and all coupling constant (*J*) values are given in Hz. IR spectra were recorded using a Bruker Tensor 27 spectrometer for samples in KBr pellets. MALDI mass spectra were acquired on a Bruker MALDI-TOF Ultraflex III spectrometer (Bruker Daltonik, Bremen, Germany). 2,5-Dihydroxybenzoic acid (5 mg ml^{-1} in methanol) was used as a matrix. Positively charged ions were registered. Elemental analysis was accomplished with an automated EuroVector EA3000 CHNS elemental analyzer (Euro-Vector, Italy). The progress of reactions and the purity of products were monitored by TLC on Sorbfil plates (IMID Ltd., Russian Federation). The TLC plates were visualized by UV. Solvents were purified and dried by standard protocols. Quinopimaric acid was prepared from levopimaric acid (from pine resin, *Pinus silvestris L.*) according to [S1].

Quantum-chemical calculations were performed using the B3PW91 hybrid density functional theory (DFT) method [S2,S3] and the extended split valence basis set TZVP [S4] with full optimization of all geometric parameters. The correspondence of the found stationary points to the energy minima was proved by calculating the second derivatives of the energy to the coordinates of the atoms, wherein all the equilibrium structures that corresponded to the minimum points on the potential energy surfaces had only positive frequency values. The calculation was carried out using the GAUSSIAN 09 software package [S5]. The calculations were carried out on the MVS-10P (MVS-10P) computing cluster of the Interdepartmental Supercomputer Center of the Russian Academy of Sciences (www.jscc.ru).

References

S1 G.F. Vafina, R.R. Fazlyev, I.M. Sakhautdinov and F.Z. Galin, *Patent RU 2371431*, 2009.

S2 A.D. Becke, *J. Chem. Phys.*, 1993, **98**, 5648.

S3 J.P. Perdew, K. Burke and Y. Wang, *Phys. Rev. B*, 1996, **54**, 16533.

S4 A. Schäfer, C. Huber and R. Ahlrichs, *J. Chem. Phys.*, 1994, **100**, 5829.

S5 M. J. Frisch, G. W. Trucks, H. B. Schlegel, G. E. Scuseria, M. A. Robb, J. R. Cheeseman, G. Scalmani, V. Barone, B. Mennucci, G. A. Petersson, H. Nakatsuji, M. Caricato, H. Li, H. P. Hratchian, A. F. Izmaylov, J. Bloino, G. Zheng, J. L. Sonnenberg, M. Hada, M. Ehara, K. Toyota, R. Fukuda, J. Hasegawa, M. Ishida, T. Nakajima, Y. Honda, O. Kitao, H. Nakai, T. Vreven, J. A. Montgomery, Jr., J. E. Peralta, F. Ogliaro, M. Bearpark, J. J. Heyd, E. Brothers, K. N. Kudin, V. N. Staroverov, R. Kobayashi, J. Normand, K. Raghavachari, A. Rendell, J. C. Burant, S. S. Iyengar, J. Tomasi, M. Cossi, N. Rega, J. M. Millam, M. Klene, J. E. Knox, J. B. Cross, V. Bakken, C. Adamo, J. Jaramillo, R. Gomperts, R. E. Stratmann, O. Yazyev, A. J. Austin, R. Cammi, C. Pomelli, J. W. Ochterski, R. L. Martin, K. Morokuma, V. G. Zakrzewski, G. A. Voth, P. Salvador, J. J. Dannenberg, S. Dapprich, A. D. Daniels, O. Farkas, J. B. Foresman, J. V. Ortiz, J. Cioslowski and D.J. Fox, *Gaussian 09, Revision A.01*, Gaussian, Wallingford, CT, 2009.

Chemistry

(7-Carboxy-7,10a-dimethyl-13-isopropyl-4,4a,5,6,6a,7,8,9,10,10a,10b,11,12,12a-hexadecahydro-1*H*-4b,12-ethenochrysen-3-yl)triphenylphosphonium trifluoroacetate (2a). Yield: 0.31 g (79 %), mp 181°C. Found, %: C 70.37, H 6.31, P 3.78. $C_{46}H_{50}F_3O_6P$. Calculated, %: C 70.22, H 6.41, P 3.94. Mass-spectrum MALDI, *m/z*: calc. for $C_{44}H_{50}O_4P^+$ [M – CF_3COO] $^+$, 673.34; found 673.70. IRS (KBr) ν_{max}, cm^{-1}: 3410, 3059, 2957, 2928, 2871, 2585, 1703, 1618, 1484, 1459, 1439, 1385, 1310, 1266, 1245, 1193, 1136, 1106, 1072, 1054, 1028, 998, 962, 887, 828, 797, 751, 719, 691, 662, 621, 600, 520, 459, 419. ^{1}H NMR spectrum ($CDCl_3$, 600 MHz, δ, ppm, *J*, Hz): 7.68 t (3H, $H^{p\text{-}Ph}$, $^3J_{HH}$ 7.1), 7.55 ddd (3H, $H^{m\text{-}Ph}$, $^3J_{HH}$ 7.1, $^3J_{HH}$ 7.1, $^3J_{HP}$ 3.3), 7.49 dd (3H, $H^{o\text{-}Ph}$, $^3J_{HH}$ 7.9, $^3J_{PH}$ 12.7), 5.45 s (1H, H^{14}), 3.51 br. s (1H, H^{12a}), 3.27 br. s (1H, H^{4a}), 2.79 d (1H, H^{3ax}, $^3J_{HH}$ 15.3), 2.53 d (1H, H^{12}, $^3J_{HH}$ 8.3), 2.31 q.q (1H, H^{15}, $^3J_{HH}$ 6.8, $^3J_{HH}$ 6.4), 2.07 dd (1H, H^{3eq}, $^3J_{HH}$ 14.0-15.0, $^3J_{PH}$ 14.0-15.0), 1.76-1.69 m (3H, H^{6a}, H^{8eq}, H^{11eq}), 1.61 dd (1H, H^{8ax}, $^3J_{HH}$ 13.6, $^4J_{HH}$ 4.5), 1.57 d (2H, H^5, $^3J_{HH}$ 12.5), 1.50 d (1H, H^{6eq}, $^3J_{HH}$ 13.8), 1.45 d (1H, H^{10eq}, $^3J_{HH}$ 14.1), 1.42 d (1H, H^{10b}, $^4J_{HH}$ 16.0), 1.37 d (2H, H^9, $^3J_{HH}$ 14.0), 1.28 d (1H, H^{6ax}, $^3J_{HH}$ 12.5) is overlapped with δ 1.26 d (1H, H^{11ax}, $^3J_{HH}$ 10.6), 1.12 s (3H, C^7–CH_3), 1.01 d (3H, C^{15}–CH_3, $^3J_{HH}$ 6.6) is overlapped with δ 1.00 d (3H, C^{15}–CH_3, $^3J_{HH}$ 6.6), 0.95 t (1H, H^{10ax}, $^3J_{HH}$ 6.6), 0.57 s (3H, C^{10a}–CH_3). ^{13}C NMR spectrum ($CDCl_3$, 126 MHz, δ_C, ppm, *J*, Hz) (the type of signal in the ^{13}C-{^{1}H} NMR spectrum is shown in parentheses): 207.05 br. s (d) (C^4, $^3J_{PC}$ 8.3), 184.35 br. s (s) (COOH), 178.81 br. s (s) (C^1), 161.05 q (q) (COO^-, $^2J_{CF}$ 34.6), 149.34 br. s (s) (C^{13}), 134.00 dtd (d) ($C^{p\text{-}Ph}$, $^1J_{HC}$ 163.8, $^2J_{HC}$ 7.5, $^4J_{PC}$ 3.1), 133.80 ddd (d) ($C^{o\text{-}Ph}$, $^1J_{HC}$ 163.8, $^2J_{HC}$ 7.1, $^3J_{PC}$ 10.7), 129.66 ddd (d) ($C^{m\text{-}Ph}$, $^1J_{HC}$ 165.2, $^2J_{HC}$ 7.1, $^3J_{PC}$ 12.7), 124.43 d (s) (C^{14}, $^1J_{HC}$ 161.8), 120.38 br. d (d) ($C^{i\text{-}Ph}$, $^1J_{PC}$ 91.3), 116.53 q (q) (CF_3, $^1J_{CF}$ 292.8), 75.10 br. d (br. d) (C^2, $^1J_{PC}$ 89.2), 59.90 d (s) (C^{12}, $^1J_{HC}$ 136.6), 55.81 d (s) (C^{10b}, $^1J_{HC}$ 127.2), 49.06 d (s) (C^{6a}, $^1J_{HC}$ 124.6), 48.61 dd (d) (C^{4a}, $^1J_{HC}$ 137.8, $^3J_{PC}$ 9.1), 46.78 s (s) (C^7), 40.97 s (s) (C^{4b}), 39.51 td (d) (C^3, $^1J_{HC}$ 132.1, $^2J_{PC}$ 6.1), 39.51 d (s) (C^{12a}, $^1J_{HC}$ 142.2) is overlapped with δ_C 37.92 s (s) (C^{10a}) and 37.79 t (s) (C^{10}, $^1J_{HC}$ 121.2) and 36.77 t (s) (C^6, $^1J_{HC}$ 120.8), 34.78 t (s) (C^5, $^1J_{HC}$ 121.9) is overlapped with δ_C 33.32 d (s) (C^{15}, $^1J_{HC}$ 125.5), 27.62 t (s) (C^8, $^1J_{HC}$ 129.4), 21.76 t (s) (C^{11}, $^1J_{HC}$ 125.0) is overlapped with δ_C 21.10 q (s) (C^{15}–CH_3, $^1J_{HC}$ 126.2) and 19.92 q (s) (C^{15}- CH_3, $^1J_{HC}$ 125.5), 16.98 t (s) (C^9, $^1J_{HC}$ 126.4) is overlapped with δ_C 16.47 q (s) (C^7–CH_3, $^1J_{HC}$ 128.5), 15.99 q (s) (C^{10a}–CH_3, $^1J_{HC}$ 122.1). ^{31}P-{^{1}H} NMR spectrum ($CDCl_3$, 162 MHz, δ_P, ppm): 20.6 (s).

(7-Carboxy-7,10a-dimethyl-13-isopropyl-4,4a,5,6,6a,7,8,9,10,10a,10b,11,12,12a-hexadecahydro-1*H*-4b,12-ethenochrysen-3-yl)tri(4-methylphenyl)phosphonium trifluoroacetate (2b). Yield: 0.32 g (77%), mp 189°C. Found, %: C 71.18, H 6.95, P 3.64. $C_{49}H_{56}F_3O_6P$. Calculated, %: C 71.00, H 6.81, F 6.88, O 11.58, P 3.74. Mass-spectrum MALDI, *m/z*: calc. for $C_{47}H_{56}O_4P^+$ [M – CF_3COO] $^+$, 715.39; found 715.40. IRS (KBr) ν_{max}, cm^{-1}: 3391, 3031, 2931, 2872, 2752, 2613, 2566, 1919, 1712, 1645, 1600, 1500, 1458, 1442, 1400, 1384, 1362, 1309, 1267, 1247, 1222, 1204, 1193, 1136, 1106, 1074, 1053, 1037, 1018, 993, 969, 961, 917, 901, 885, 831, 807, 766, 719, 707, 668, 653, 633, 623, 602, 573, 545, 514, 477, 454, 433, 422, 411. ^{1}H NMR spectrum ($CDCl_3$, 400 MHz, δ, ppm, *J*, Hz): 7.42 – 7.28 m (12H, $H^{o\text{-}Ph}$ is overlapped with $H^{m\text{-}Ph}$), 5.42 s (1H, H^{14}), 3.57 br. d (1H, H^{12a}, $^3J_{HH}$ 8.4), 3.33 br. s (1H, H^{4a}), 2.75 d (1H, H^{3ax}, $^3J_{HH}$ 14.7), 2.53 d (1H, H^{12}, $^3J_{HH}$ 9.3), 2.44 s (9H, $H^{Ph\text{-}Me}$), 2.34 q.q (1H, H^{15}, $^3J_{HH}$ 6.6, $^3J_{HH}$ 6.5), 2.05 dd (1H, H^{3eq}, $^3J_{HH}$ 13.0-15.0, $^3J_{PH}$ 13.0-15.0), 1.91-1.69 m (3H, H^{6a}, H^{8eq}, H^{11eq}), 1.67-1.32 m (8H, H^{8ax}, H^5, H^{6eq}, H^{10eq}, H^{10b}, H^9), 1.26 d (1H, H^{6ax}, $^3J_{HH}$ 11.4), 1.15 d (1H, H^{11ax}, $^3J_{HH}$ 14.0), 1.13 s (3H, C^7-CH_3), 1.03 d (3H, C^{15}-CH_3, $^3J_{HH}$ 6.9), 1.01 d (3H, C^{15}-CH_3, $^3J_{HH}$ 6.9), 0.95-0.84 m (1H, H^{10ax}), 0.57 s (3H, C^{10a}-CH_3). ^{13}C NMR spectrum ($CDCl_3$, 101 MHz, δ_C, ppm, *J*, Hz) (the type of signal in the ^{13}C-{^{1}H} NMR spectrum is shown in parentheses): 207.09 br. s (d) (C^4, $^3J_{CP}$ 7.1), 183.89 s (s) (COOH), 177.36 br. s (d) (C^1, $^2J_{CP}$ 12.1), 160.83 q (q) (COO^-, $^2J_{CF}$ 35.1), 149.11 br. s (s) (C^{13}), 144.75 d (s) ($C^{p\text{-}Ph}$, $^2J_{HC}$ 4.2), 133.51 ddd (d) ($C^{o\text{-}Ph}$, $^1J_{HC}$ 162.9, $^2J_{HC}$ 6.4, $^3J_{CP}$ 10.1), 130.12 ddd (d) ($C^{m\text{-}Ph}$, $^1J_{HC}$ 159.2, $^2J_{HC}$ 5.0, $^3J_{CP}$ 13.0), 124.15 d (s) (C^{14}, $^1J_{HC}$ 159.2), 117.01 br. d (d) ($C^{i\text{-}Ph}$, $^1J_{CP}$ 93.6), 116.45 q (q) (CF_3, $^1J_{CF}$ 293.4), 76.17 br. d (br. d) (C^2, $^1J_{CP}$ 94.2), 59.76 d (s) (C^{12}, $^1J_{HC}$ 133.0), 55.67 d (s) (C^{10b}, $^1J_{HC}$ 125.7), 48.88 d (s) (C^{6a}, $^1J_{HC}$ 119.7), 48.38 dd (d) (C^{1a}, $^1J_{HC}$ 135.1, $^3J_{CP}$ 7.8), 46.54 s (s) (C^7), 40.72 s (s) (C^{4b}), 39.35 td (d) (C^3, $^1J_{HC}$ 135.2, $^2J_{CP}$ 5.4), 38.19 d (s) (C^{4a}, $^1J_{HC}$ 105.5), 37.73 s (s) (C^{10a}) is overlapped with 37.52 t (s) (C^{10}) and 36.59 t (s) (C^8), 34.59 t (s) (C^5, $^1J_{HC}$ 116.3), 33.14 d (s) (C^{15}, $^1J_{HC}$ 125.0), 27.39 t (s) (C^{11}, $^1J_{HC}$ 128.4), 21.56 t (s) (C^6, $^1J_{HC}$ 128.9) is overlapped with 21.42 q (s) ($C^{Ph\text{-}CH3}$, $^1J_{HC}$ 127.76), 20.90 q (s) (C^{15}- CH_3, $^1J_{HC}$ 124.3), 19.72 q (s) (C^{15}- CH_3, $^1J_{HC}$ 124.3), 16.78 t (s) (C^9, $^1J_{HC}$ 125.3), 16.30 q (s) (C^7- CH_3, $^1J_{HC}$ 130.3) is overlapped with 15.80 q (s) (C^{10a}-CH_3, $^1J_{HC}$ 123.0). ^{31}P-{^{1}H} NMR spectrum ($CDCl_3$, 162 MHz, δ_P, ppm): 19.8 (s).

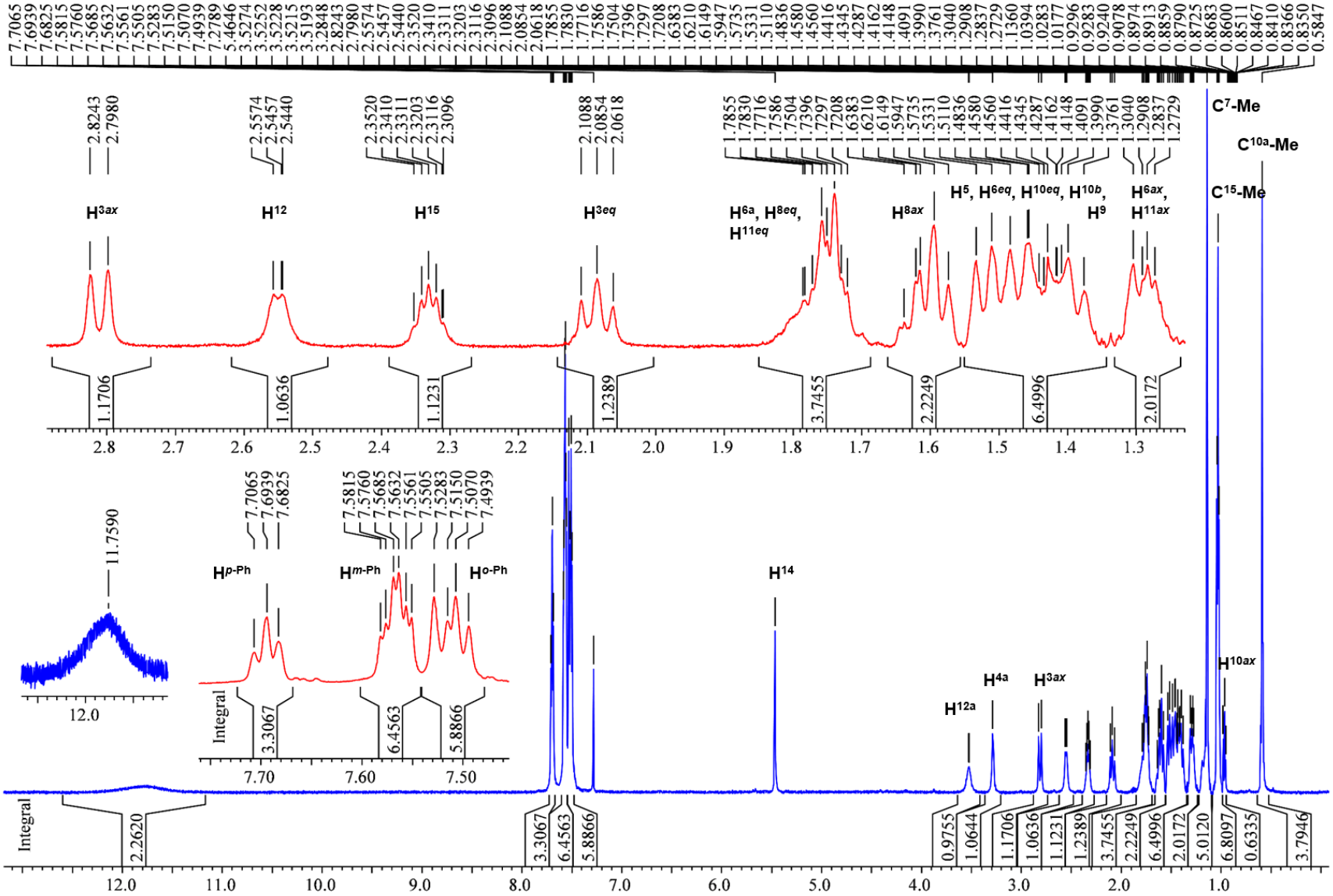

Figure S1. ^{1}H NMR ($CDCl_3$, 600 MHz) spectrum of phosphonium salt **2a**.

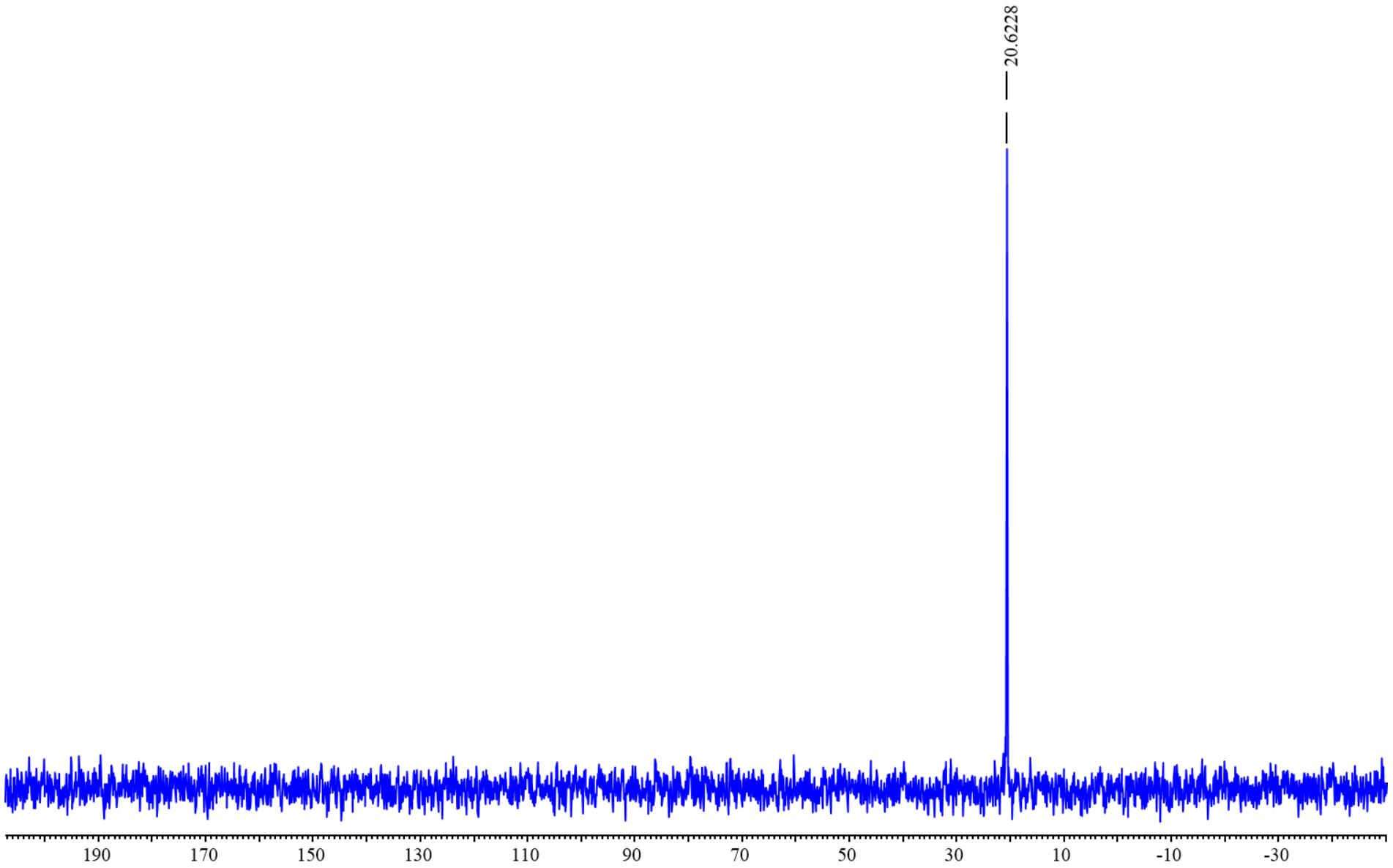

Figure S2. ^{31}P NMR ($CDCl_3$, 162 MHz) spectrum of phosphonium salt **2a**.

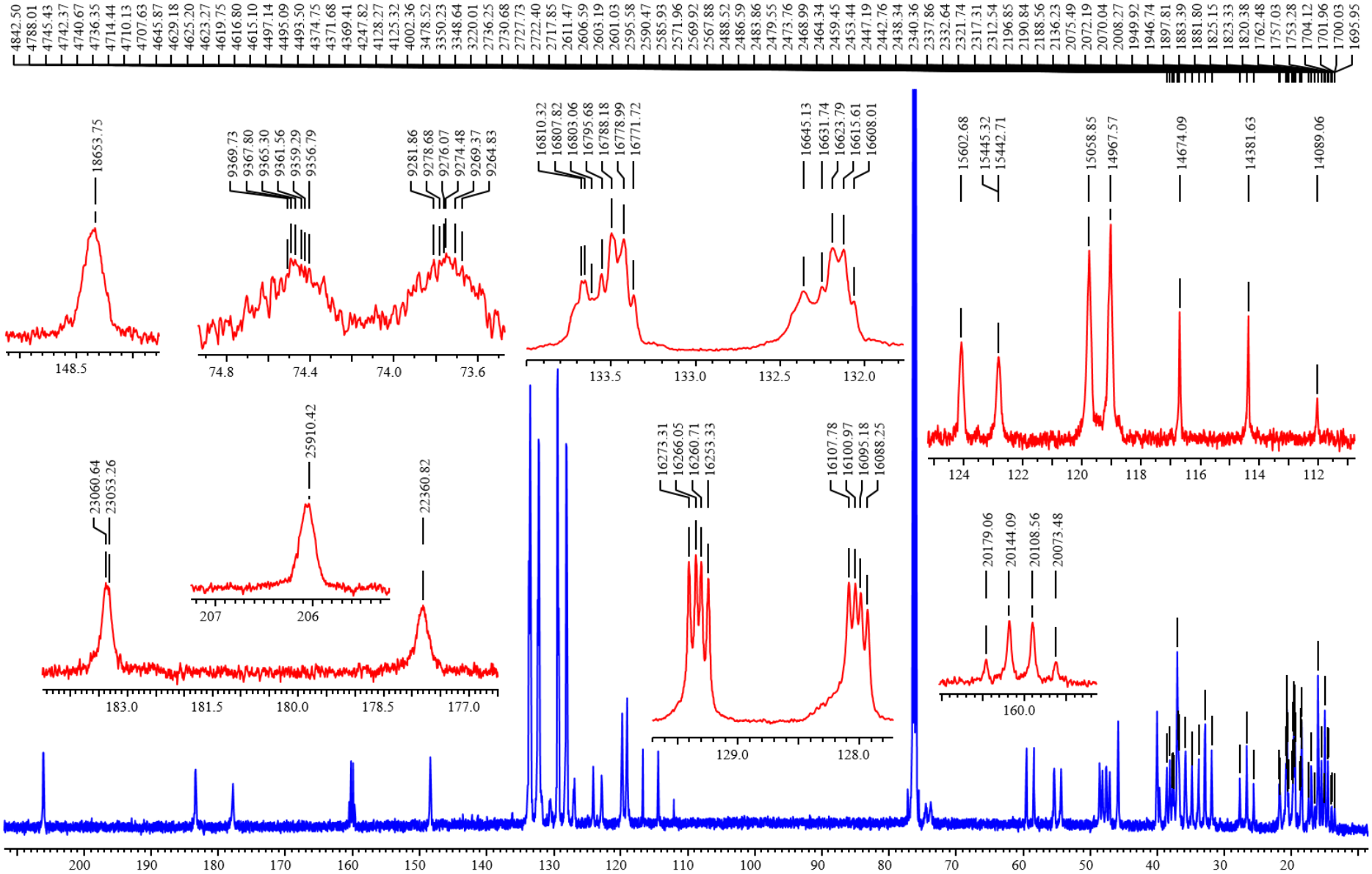

Figure S3. ^{13}C NMR ($CDCl_3$, 126 MHz) spectrum of phosphonium salt **2a**.

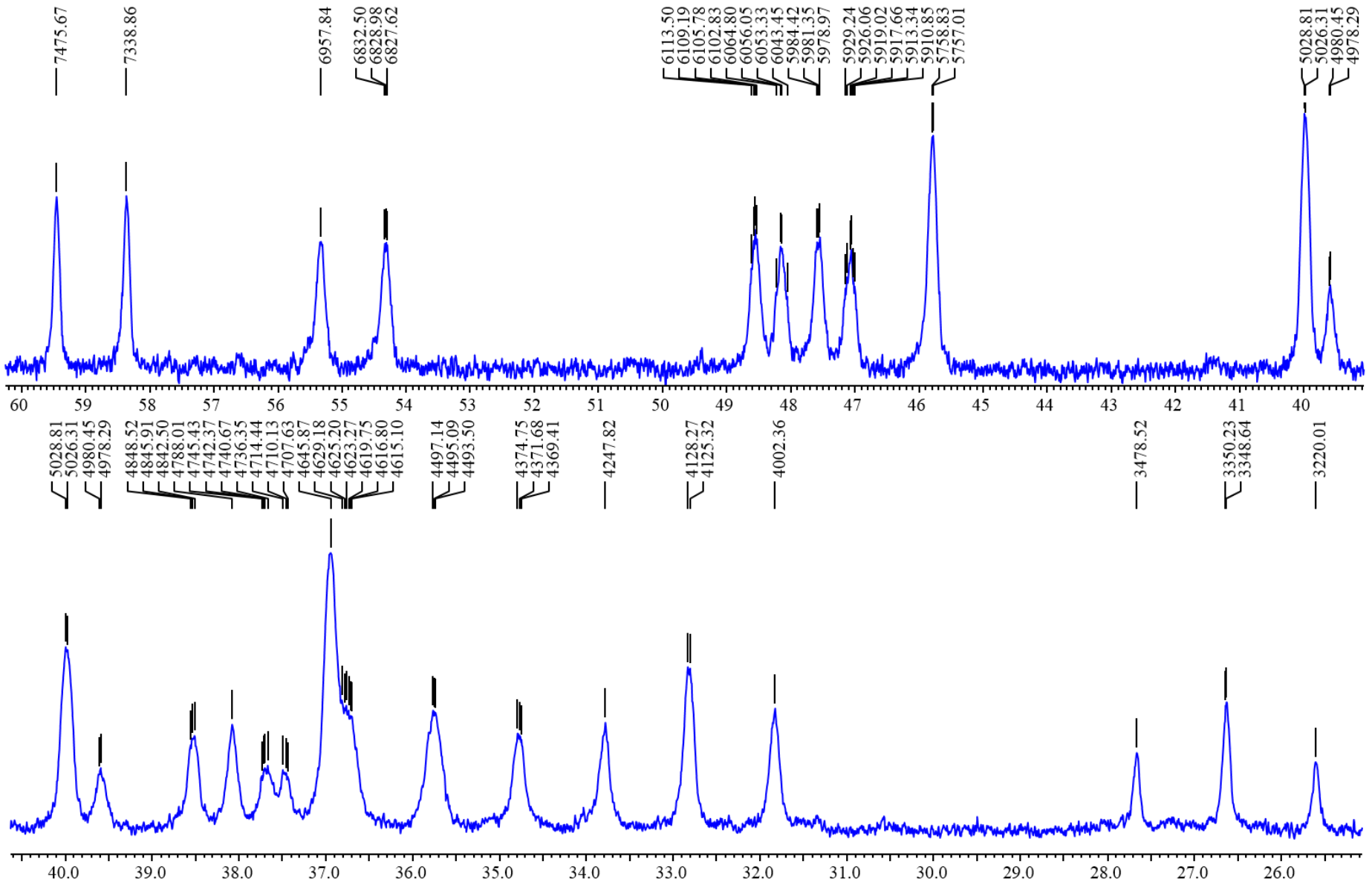

Figure S4. Fragment (60-25 ppm) of ^{13}C NMR ($CDCl_3$, 126 MHz) spectrum of phosphonium salt **2a**.

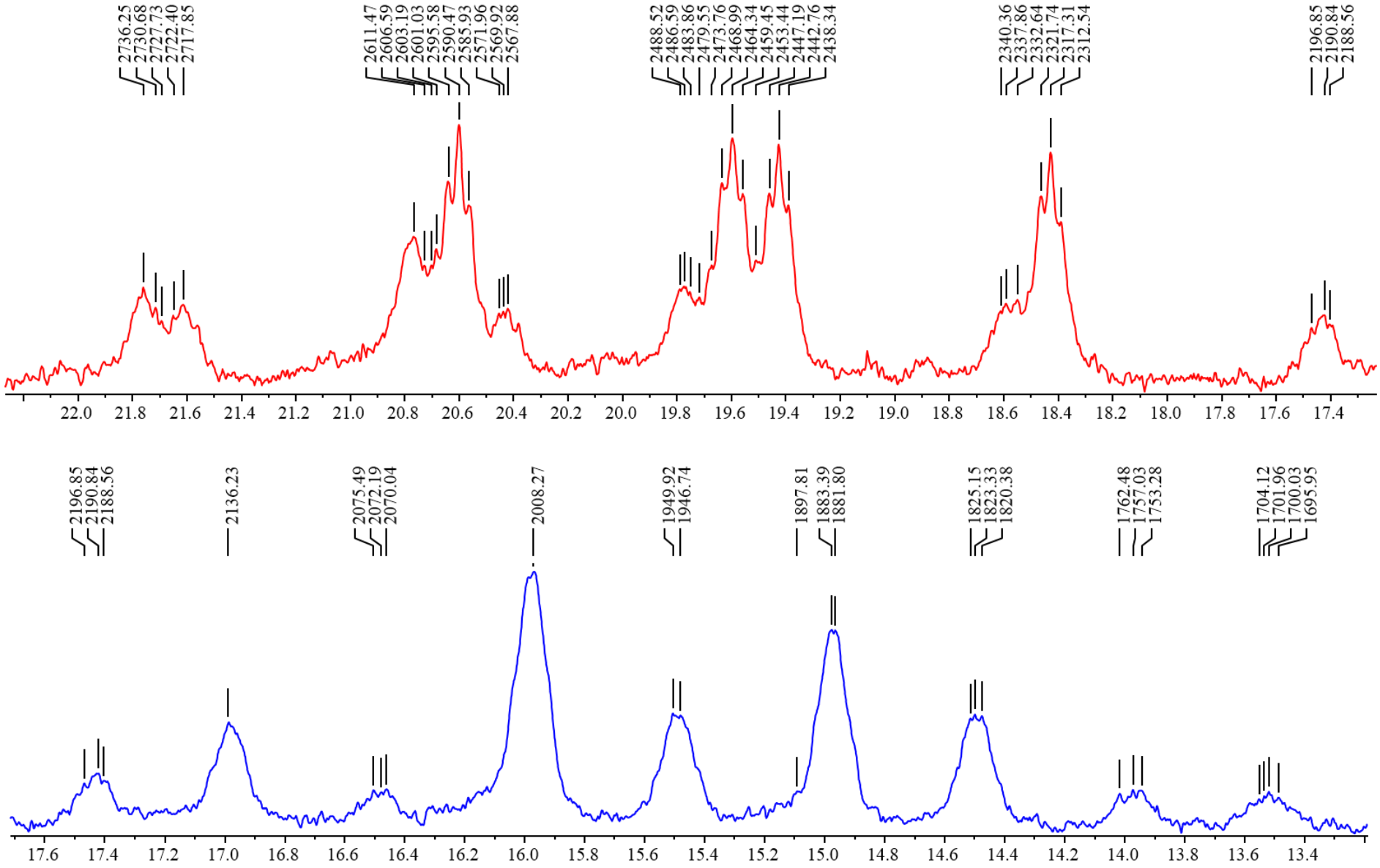

Figure S5. Fragment (22-13 ppm) of ^{13}C NMR ($CDCl_3$, 126 MHz) spectrum of phosphonium salt **2a**.

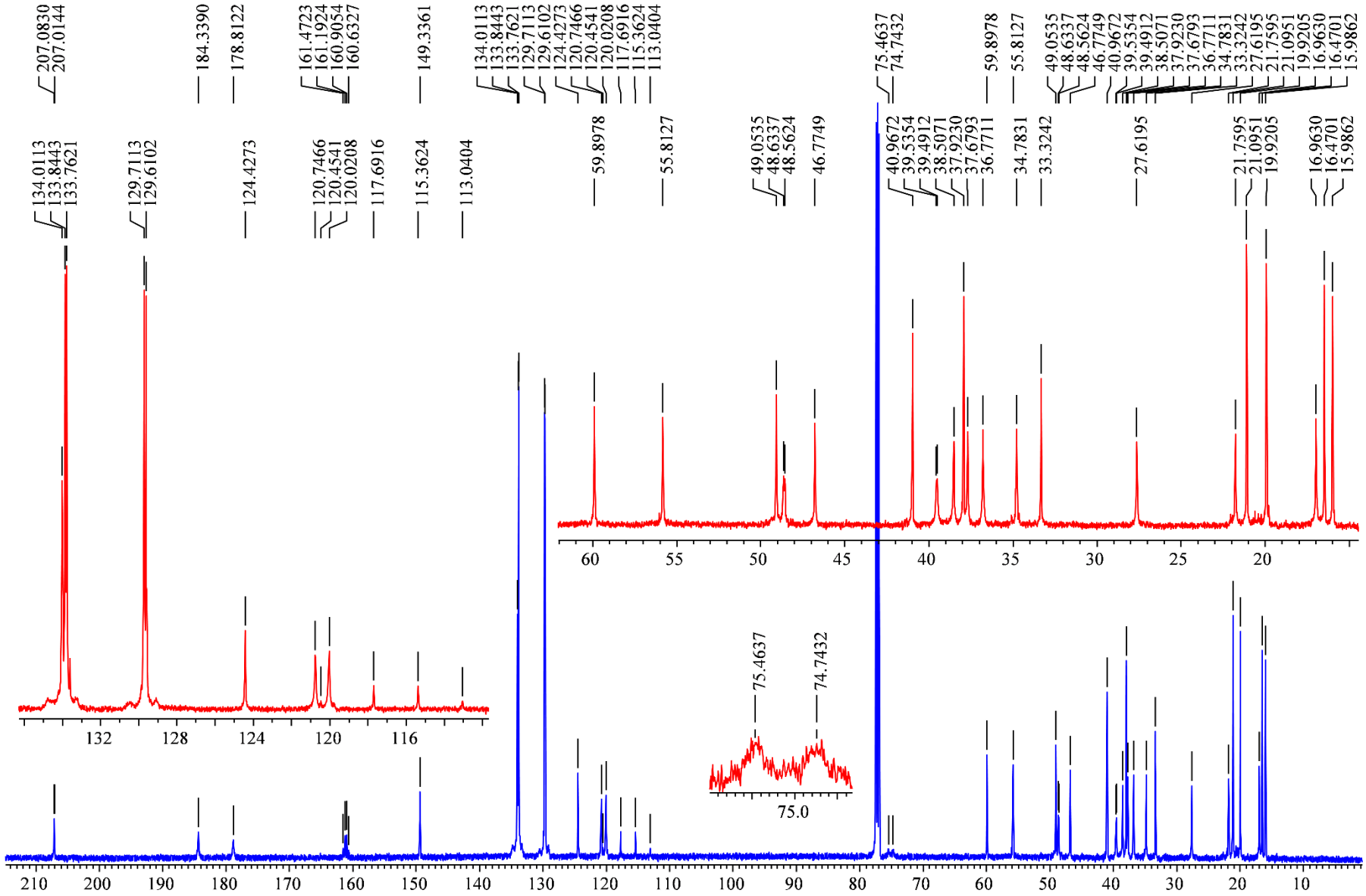

Figure S6. $^{13}C–\{^{1}H\}$ NMR ($CDCl_3$, 126 MHz) spectrum of phosphonium salt **2a**.

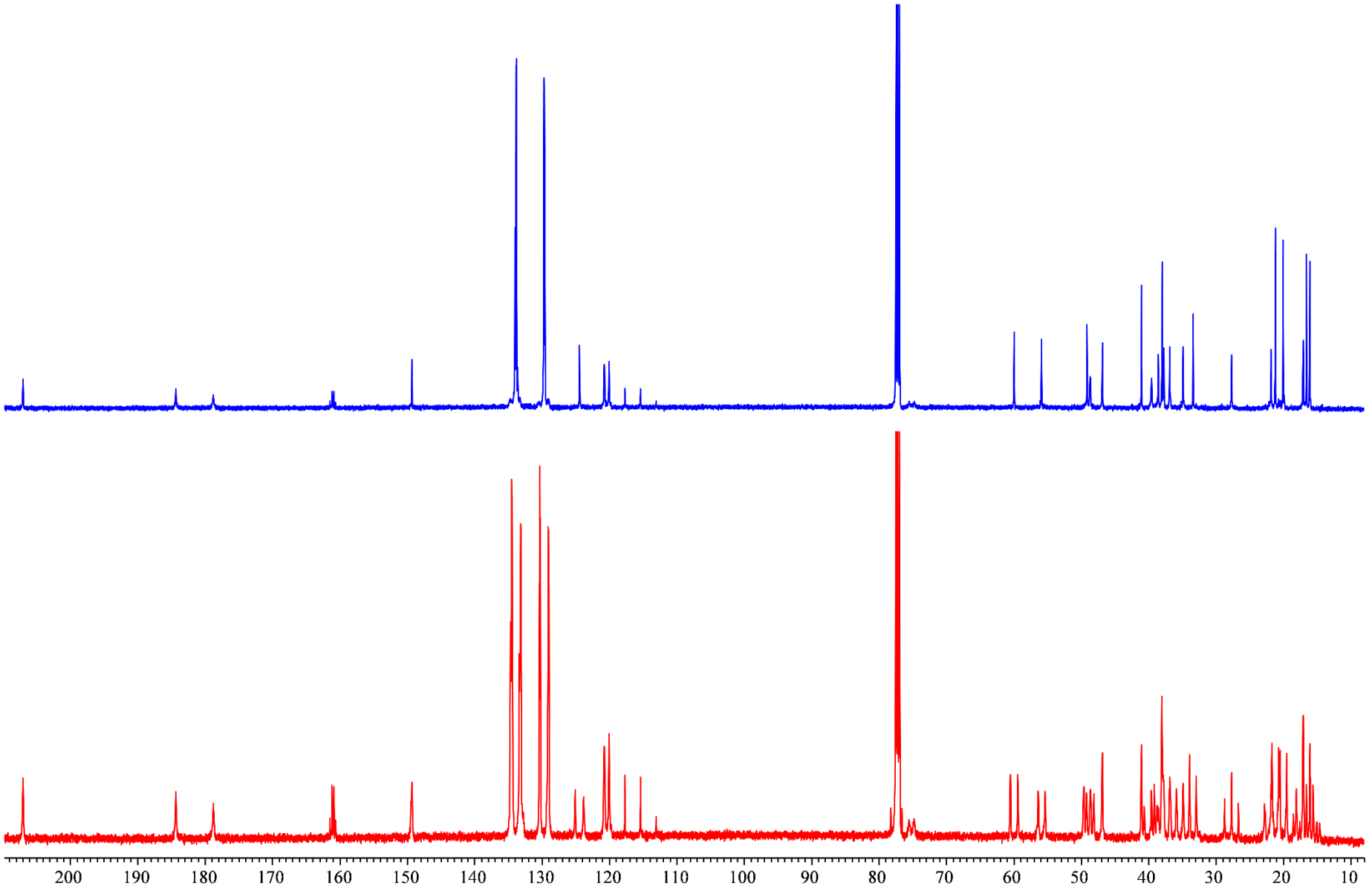

Figure S7. Comparison of $^{13}C–\{^{1}H\}$ and ^{13}C NMR ($CDCl_3$, 126 MHz) spectra of phosphonium salt **2a**.

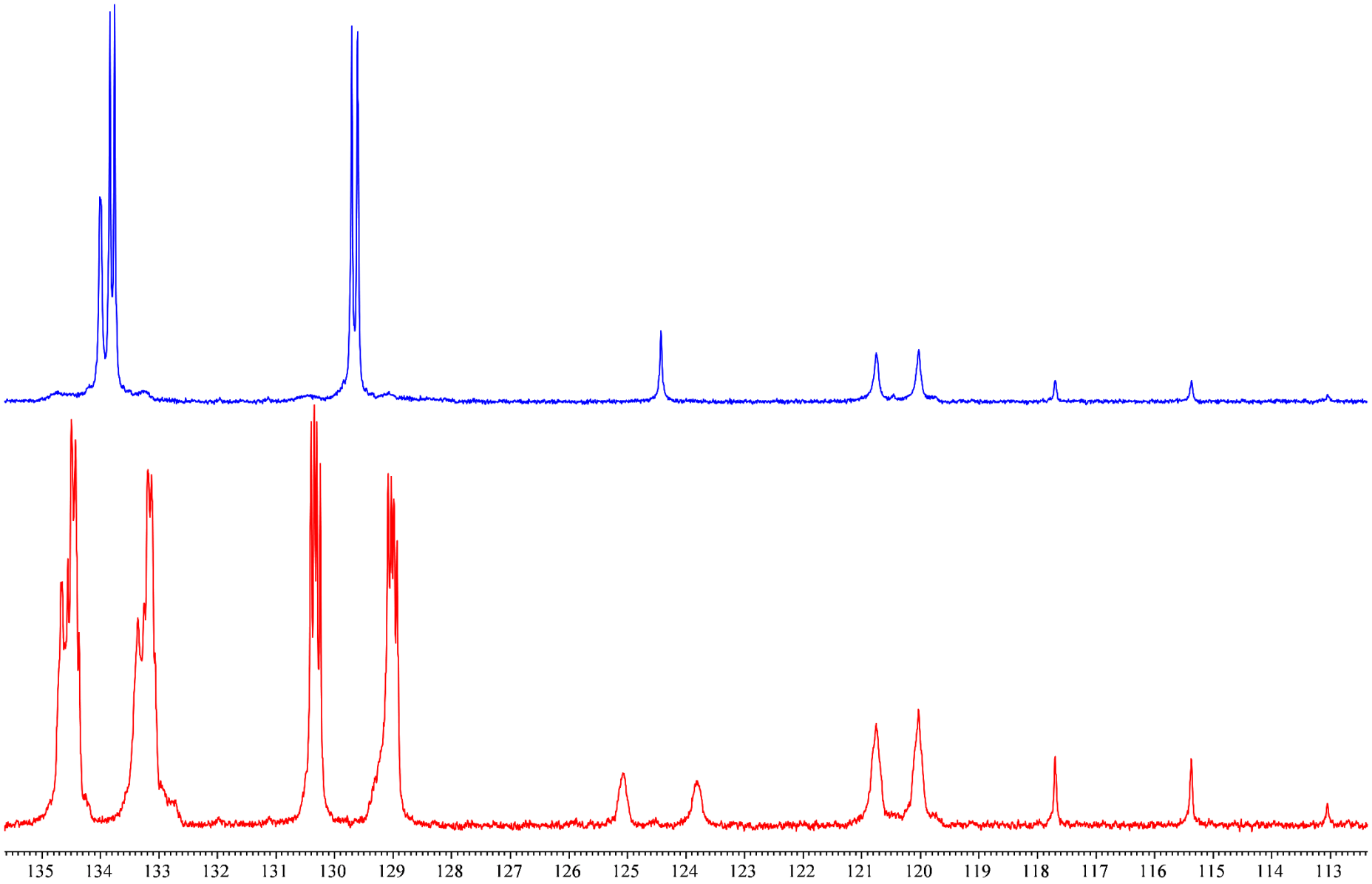

Figure S8. Fragment (δ_C 135-113 ppm) of $^{13}C–\{^1H\}$ and ^{13}C NMR ($CDCl_3$, 126 MHz) spectra of phosphonium salt **2a**.

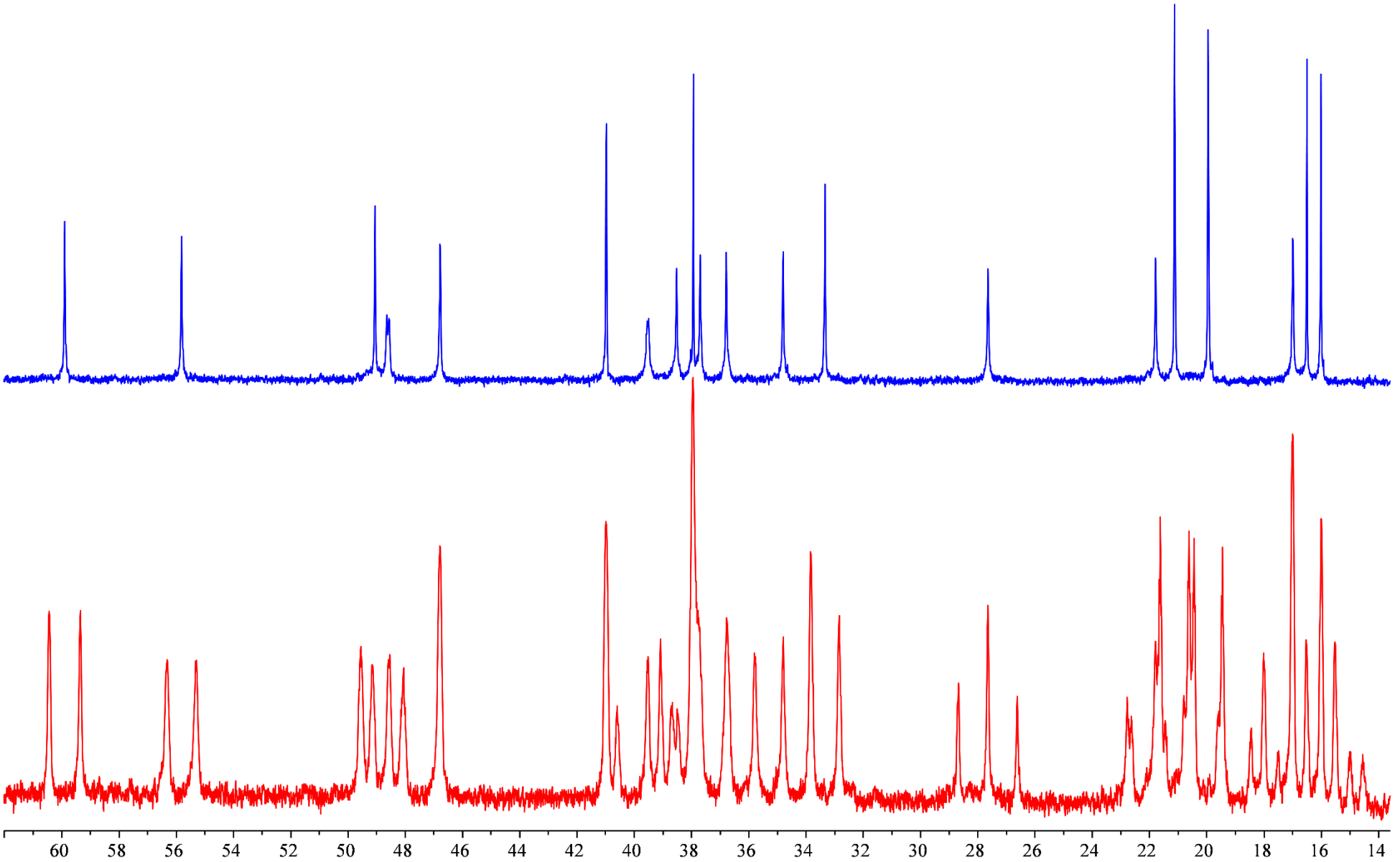

Figure S9. Fragment (δ_C 62-12 ppm) of $^{13}C–\{^1H\}$ and ^{13}C NMR ($CDCl_3$, 126 MHz) spectra of phosphonium salt **2a**.

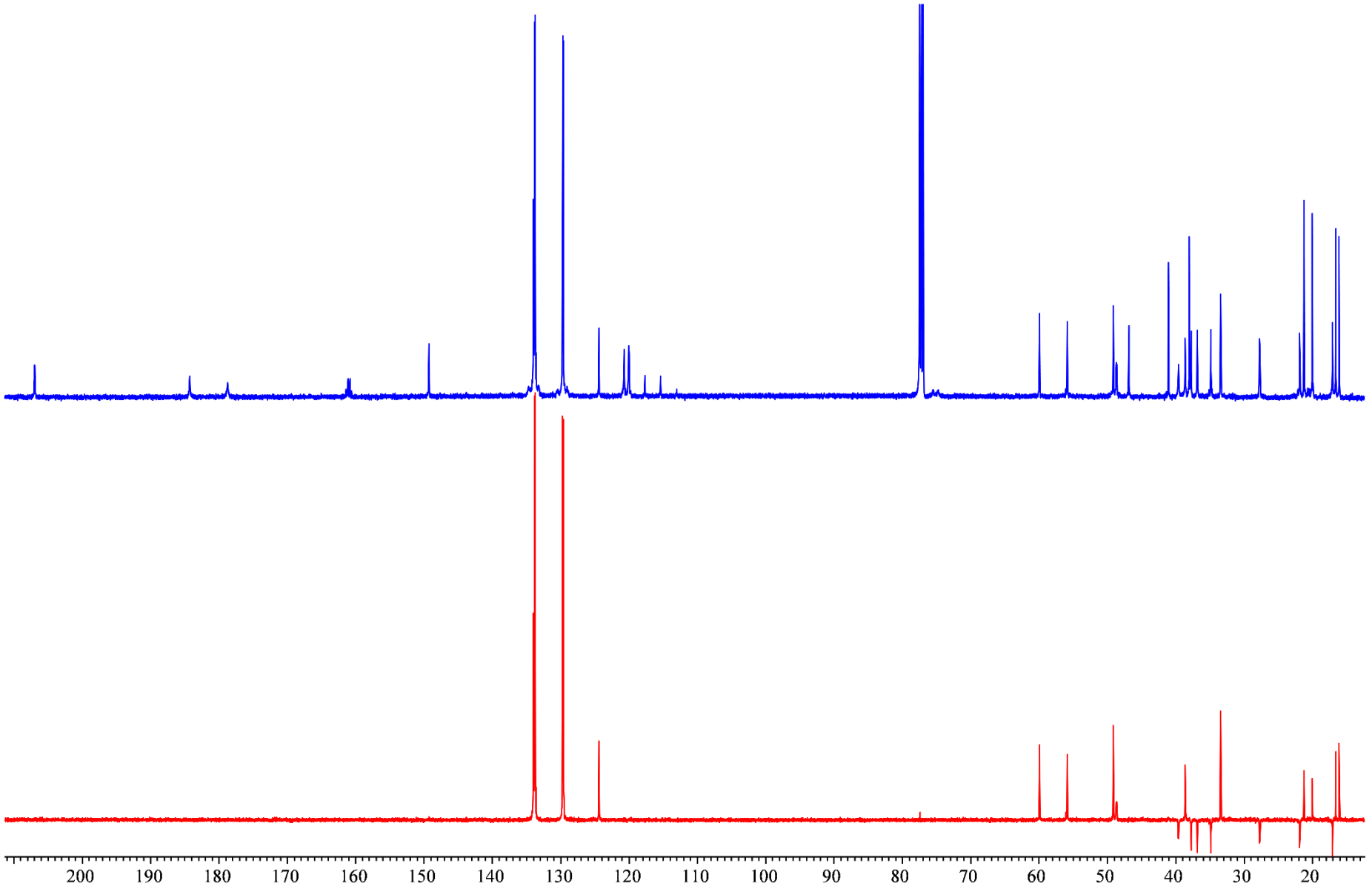

Figure S10. Comparison of $^{13}C–\{^{1}H\}$ and $^{13}C–\{^{1}H\}$-dept NMR ($CDCl_3$, 126 MHz) spectra of phosphonium salt **2a**.

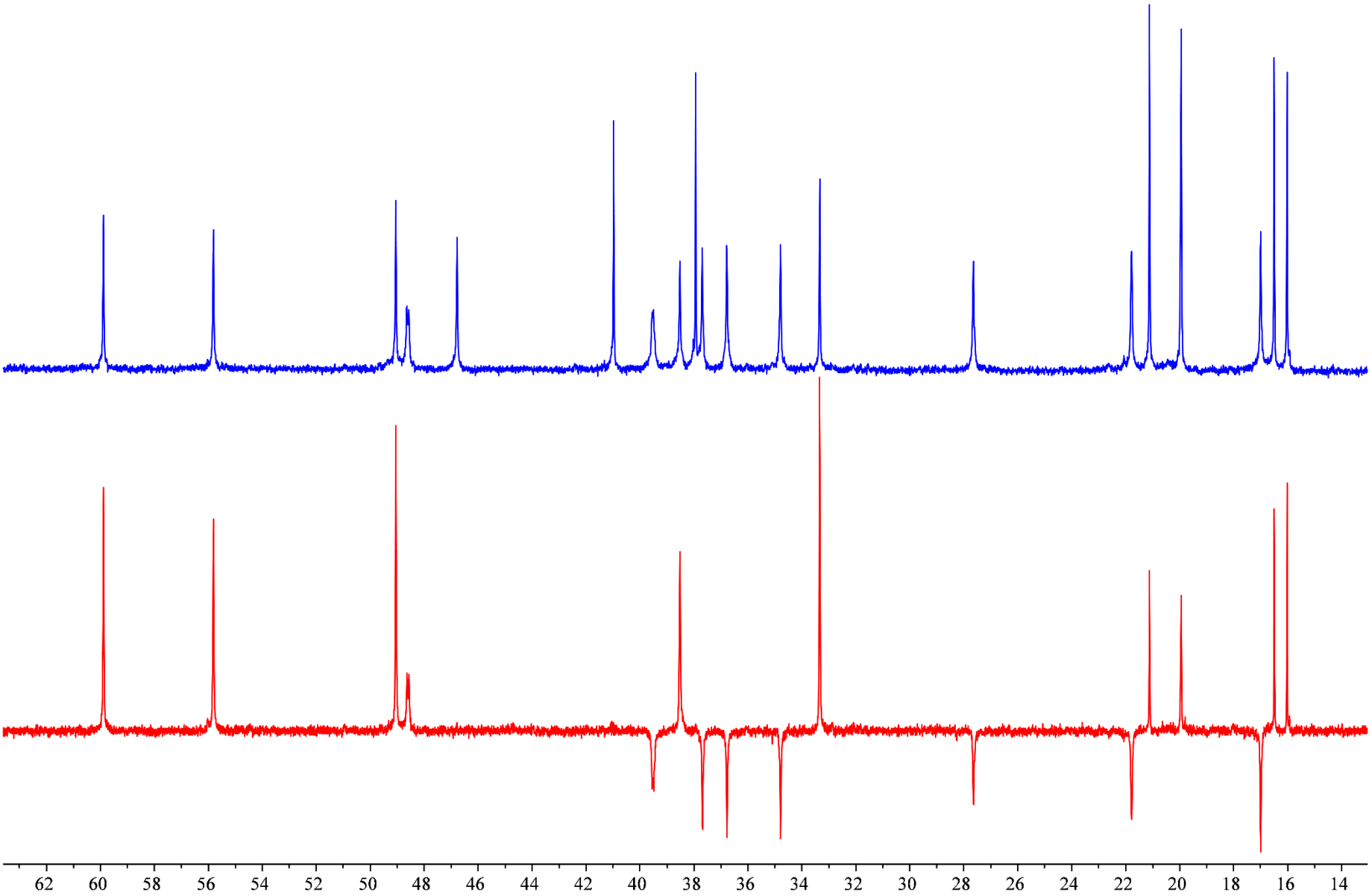

Figure S11. Fragment (δ_C 62-14 ppm) of $^{13}C–\{^1H\}$ and $^{13}C–\{^1H\}$-dept NMR ($CDCl_3$, 126 MHz) spectra of phosphonium salt **2a**.

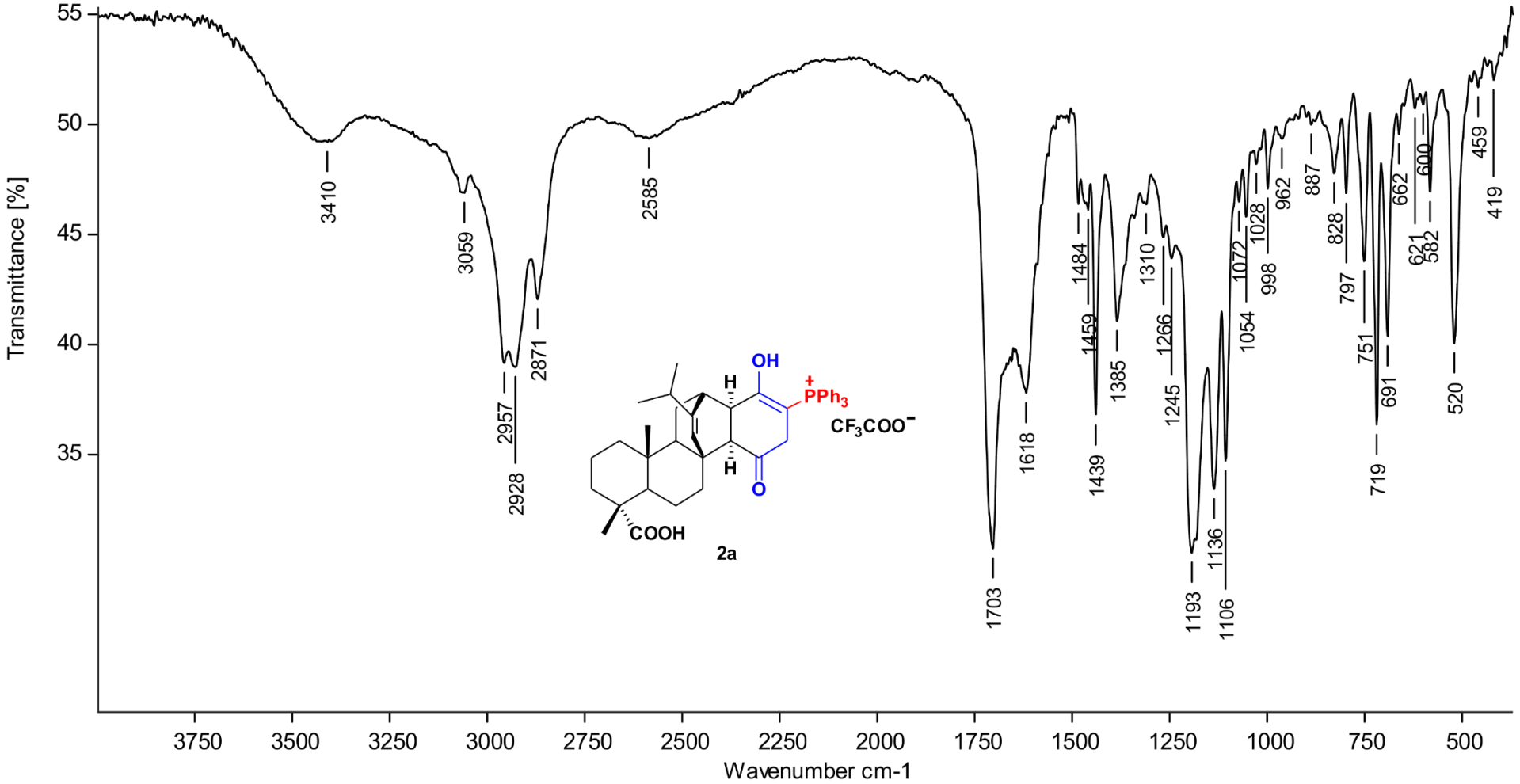

Figure S12. IR (KBr) spectrum of phosphonium salt **2a**.

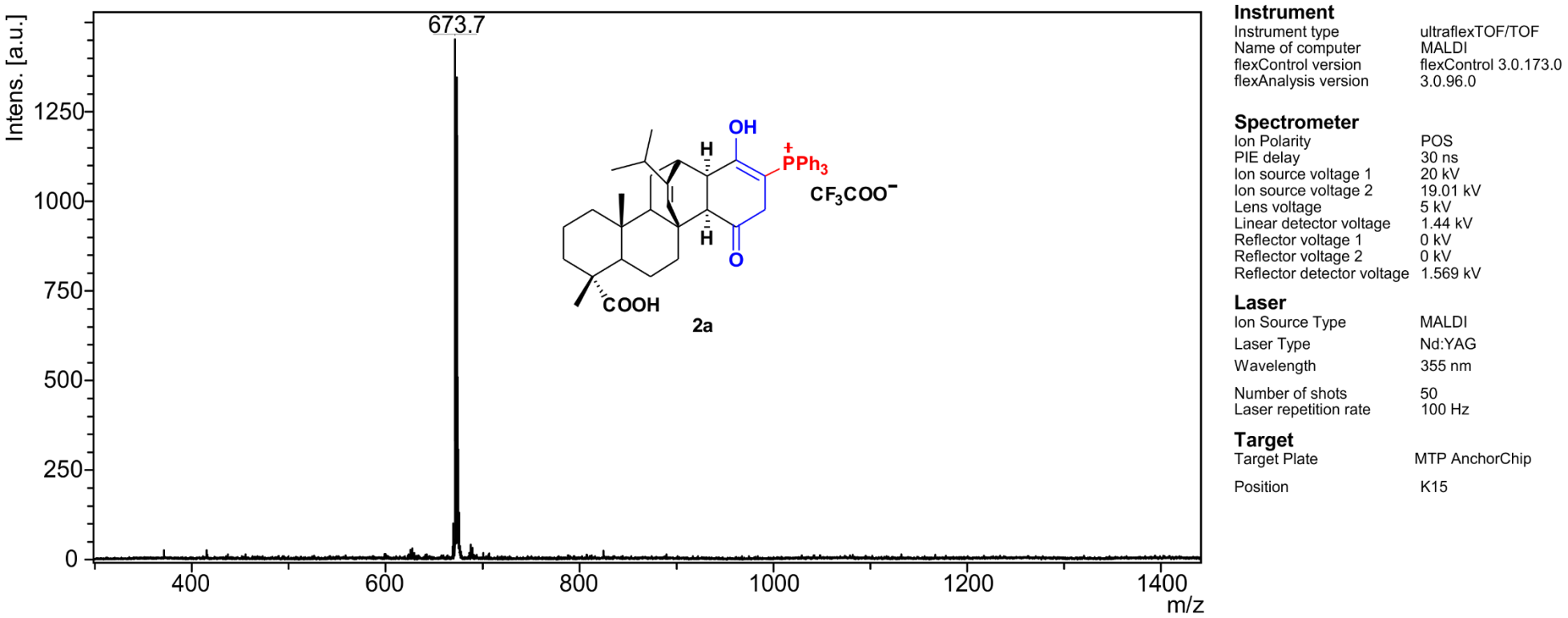

Figure S13. MALDI MS spectrum of phosphonium salt **2a**.

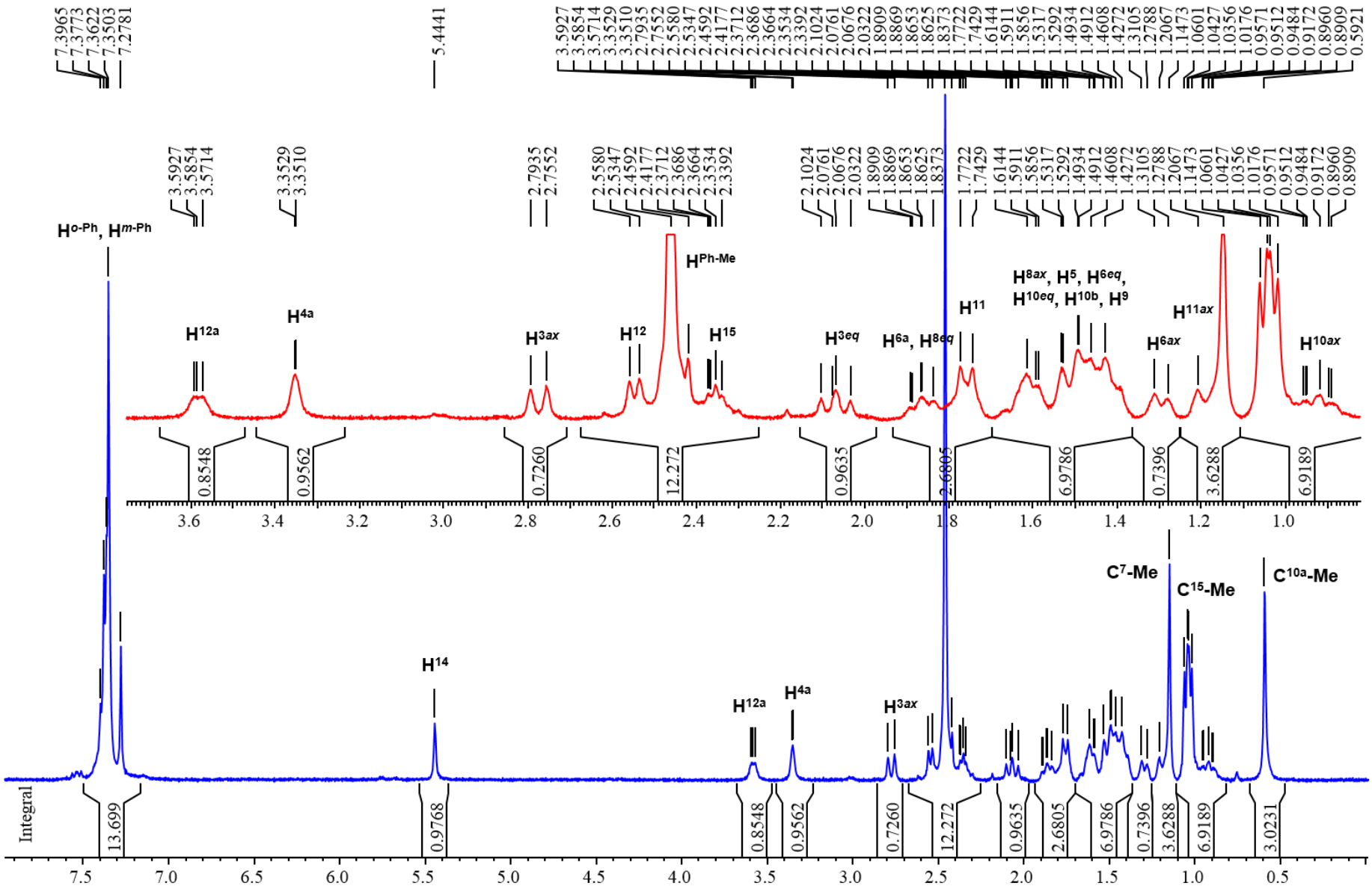

Figure S14. ^{1}H NMR ($CDCl_3$, 400 MHz) spectrum of phosphonium salt **2b**.

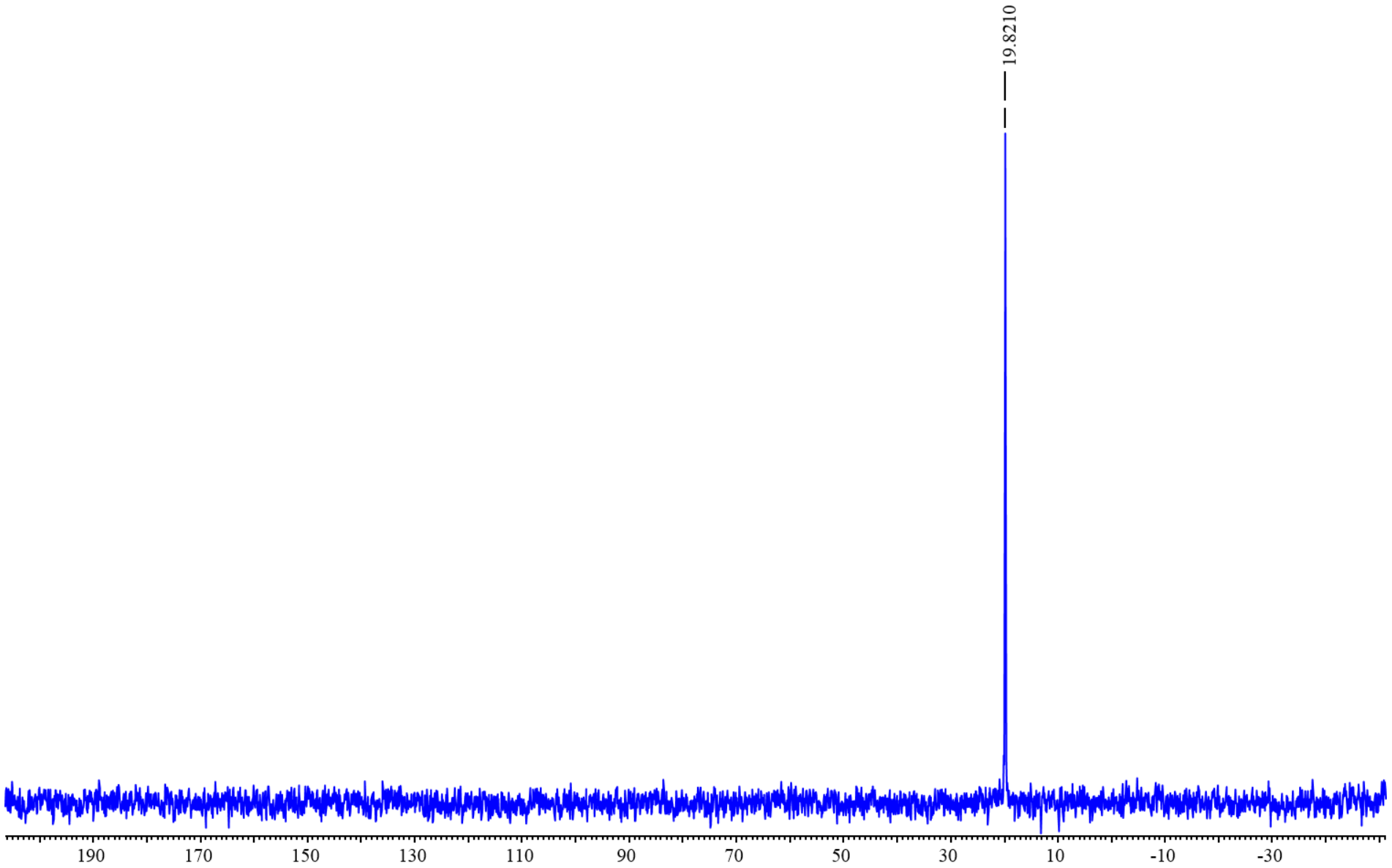

Figure S15. ^{31}P NMR ($CDCl_3$, 162 MHz) spectrum of phosphonium salt **2b**.

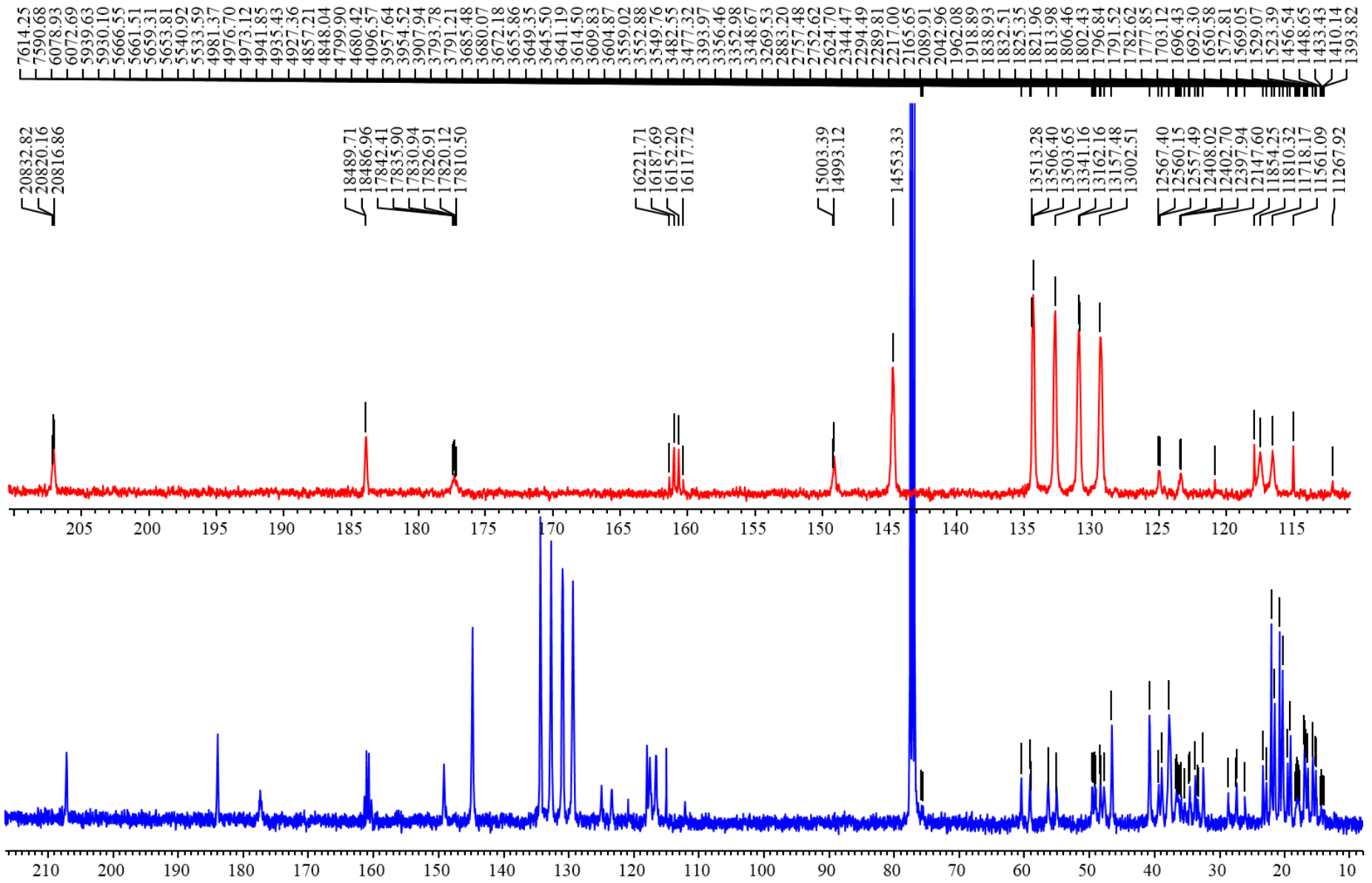

Figure S16. ^{13}C NMR ($CDCl_3$, 101 MHz) spectrum of phosphonium salt **2b**.

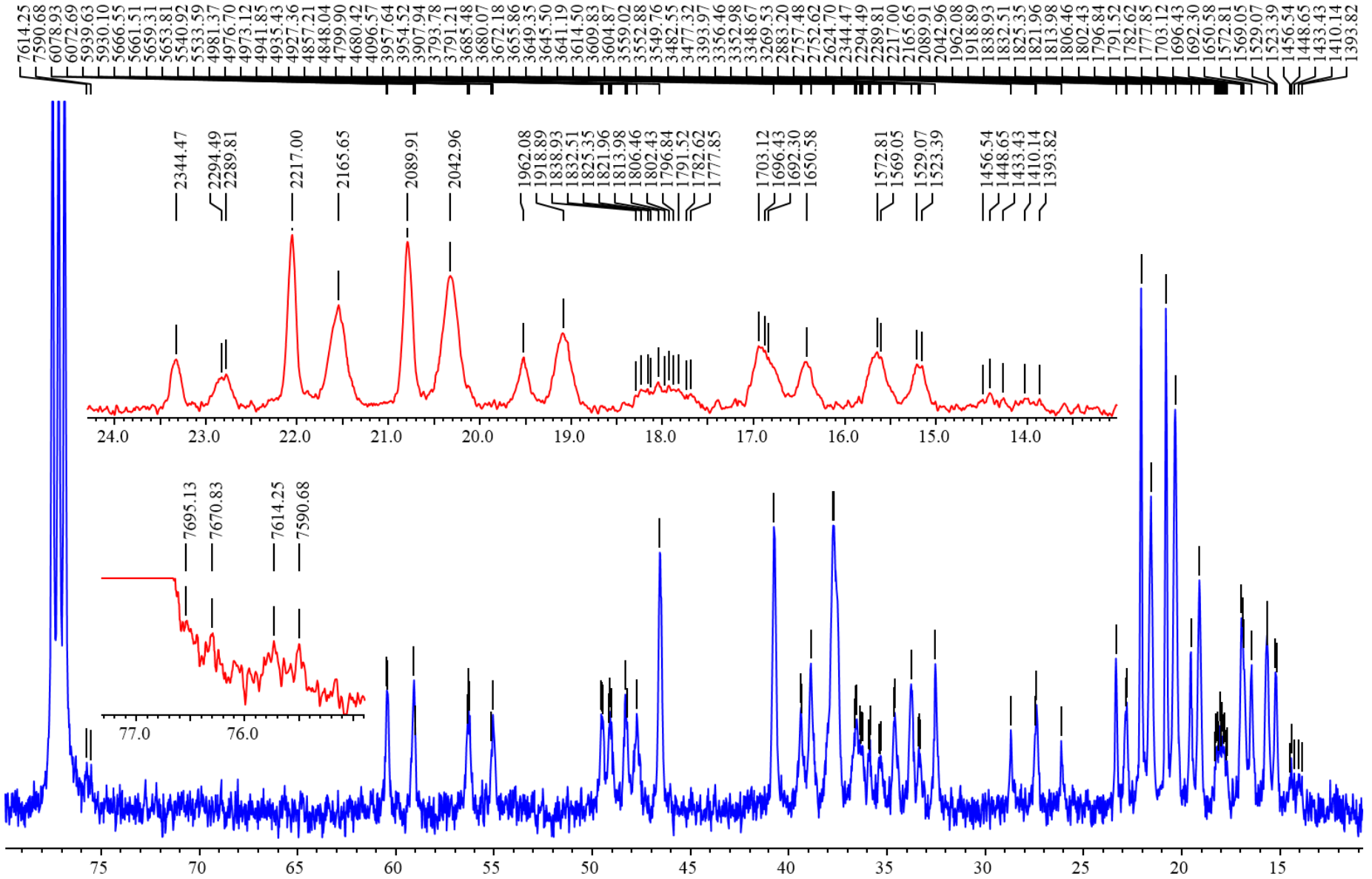

Figure S17. Fragment (δ_C 80-14 ppm) of ^{13}C NMR ($CDCl_3$, 101 MHz) spectrum of phosphonium salt **2b**.

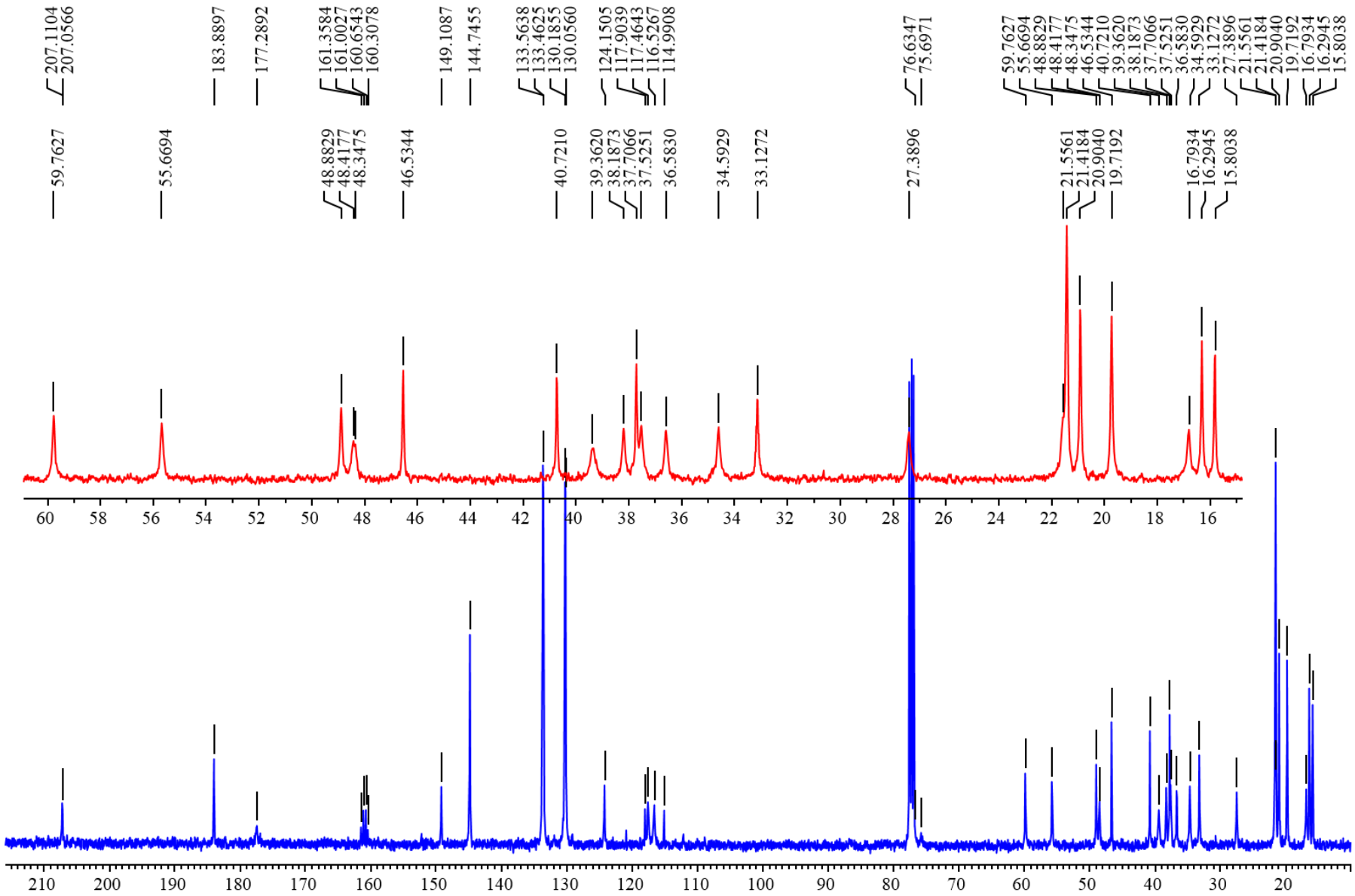

Figure S18. $^{13}C–\{^{1}H\}$ NMR ($CDCl_3$, 101 MHz) spectrum of phosphonium salt **2b**.

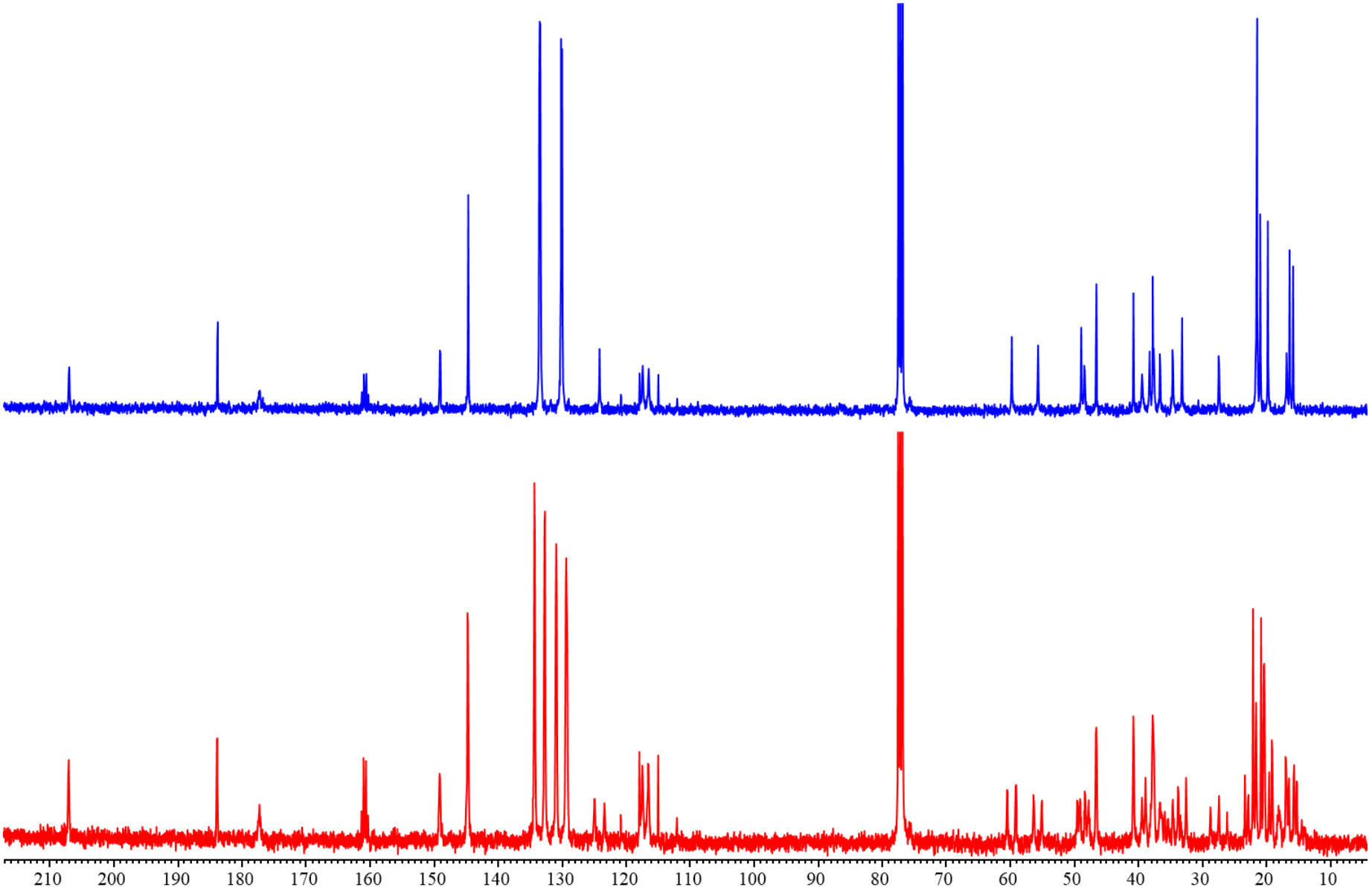

Figure S19. Comparison of $^{13}C–\{^{1}H\}$ and ^{13}C NMR ($CDCl_3$, 101 MHz) spectra of phosphonium salt **2b**.

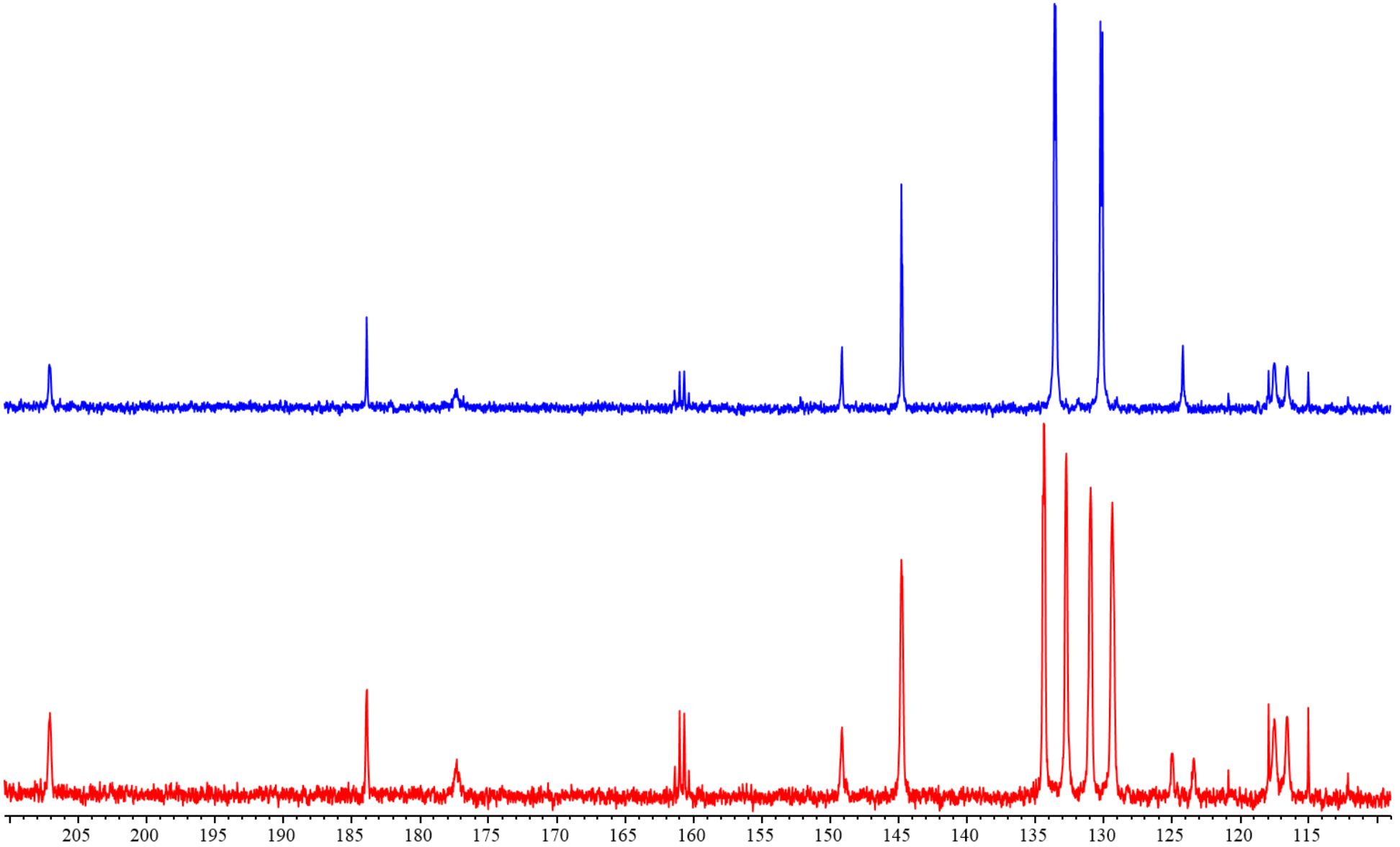

Figure S20. Fragment (δ_C 210-110 ppm) of $^{13}C–\{^1H\}$ and ^{13}C NMR ($CDCl_3$, 101 MHz) spectra of phosphonium salt **2b**.

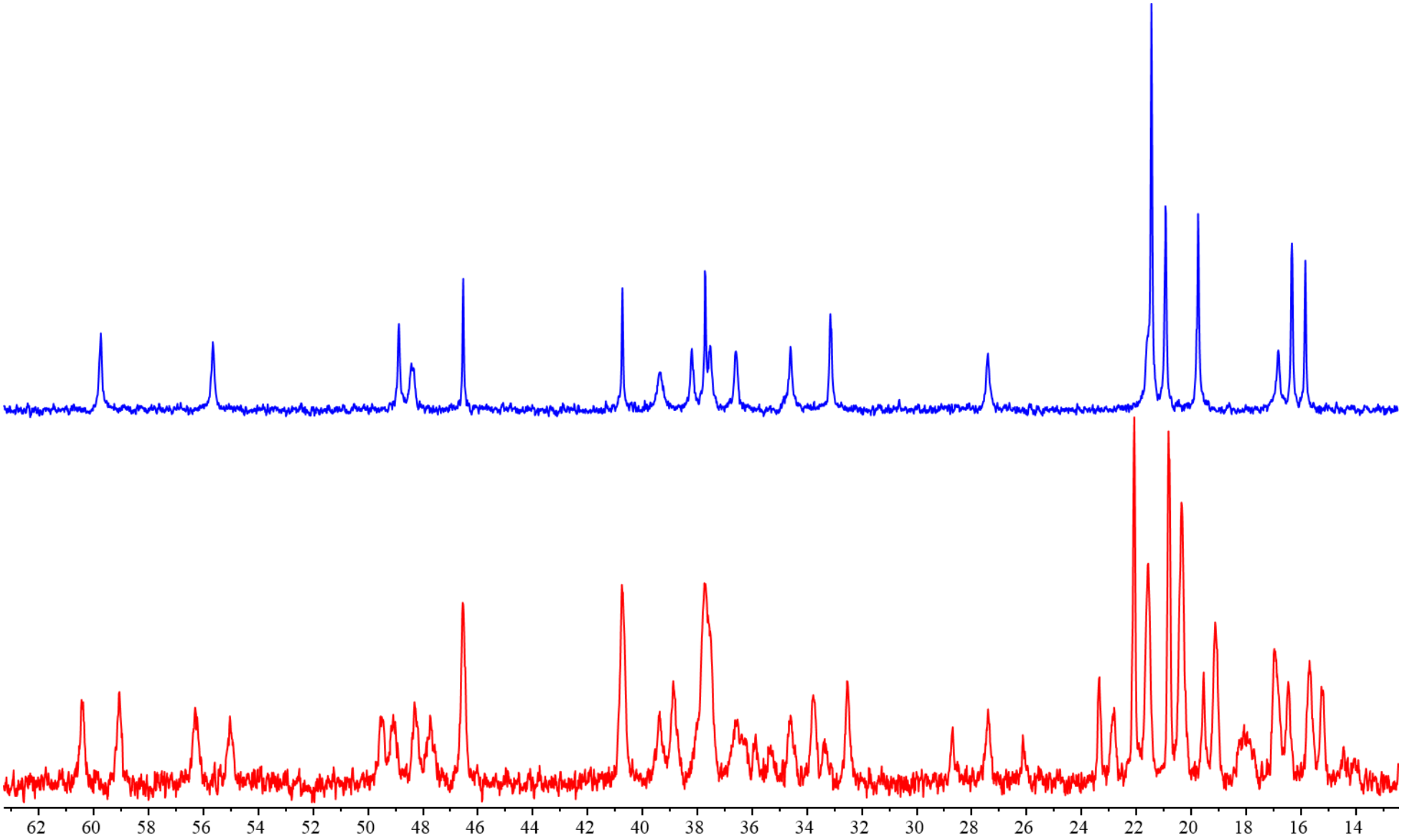

Figure S21. Fragment (δ_C 62-12 ppm) of $^{13}C–\{^1H\}$ and ^{13}C NMR ($CDCl_3$, 101 MHz) spectra of phosphonium salt **2b**.

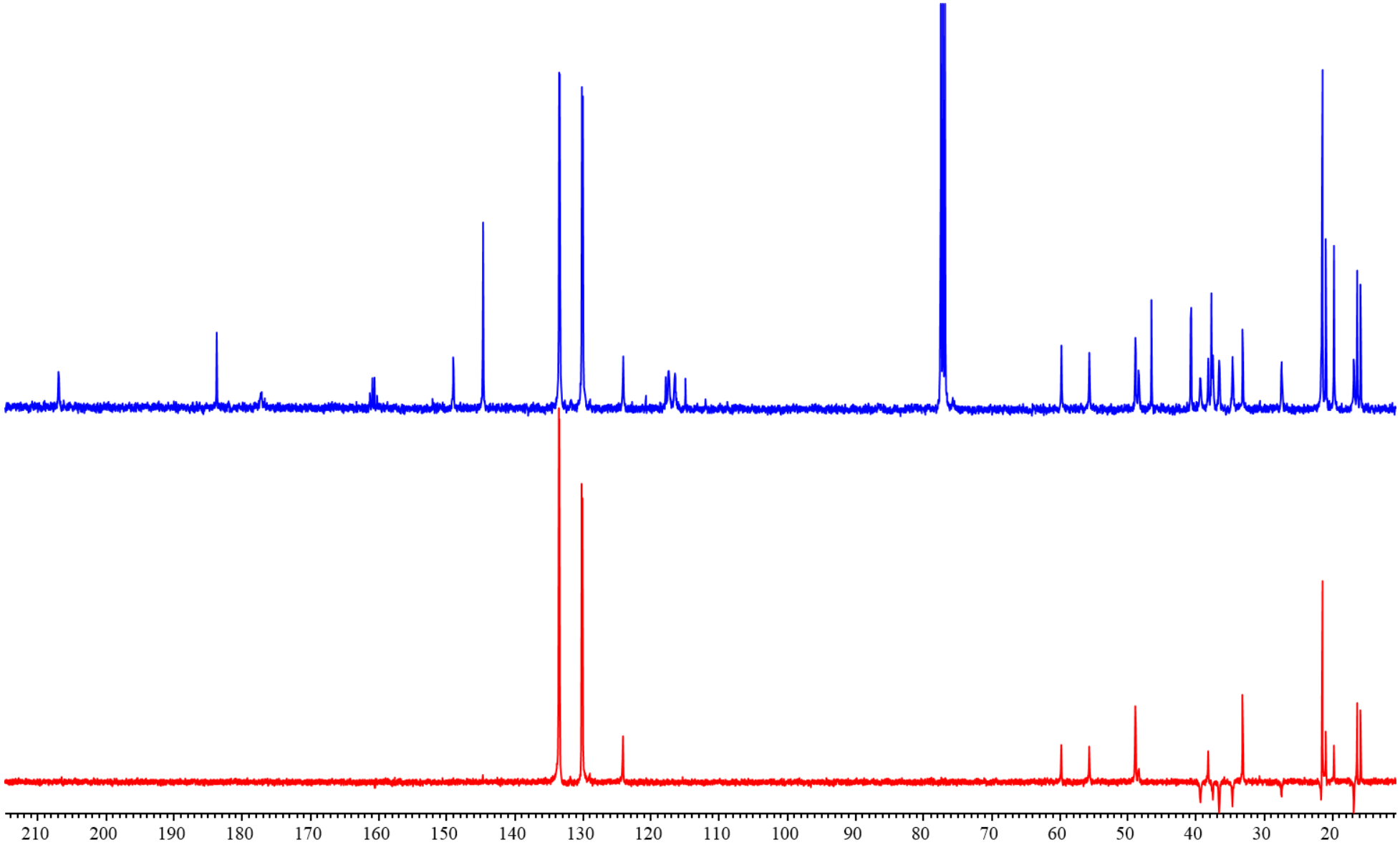

Figure S22. Comparison of $^{13}C–\{^{1}H\}$ and $^{13}C–\{^{1}H\}$-dept NMR ($CDCl_3$, 101 MHz) spectra of phosphonium salt **2b**.

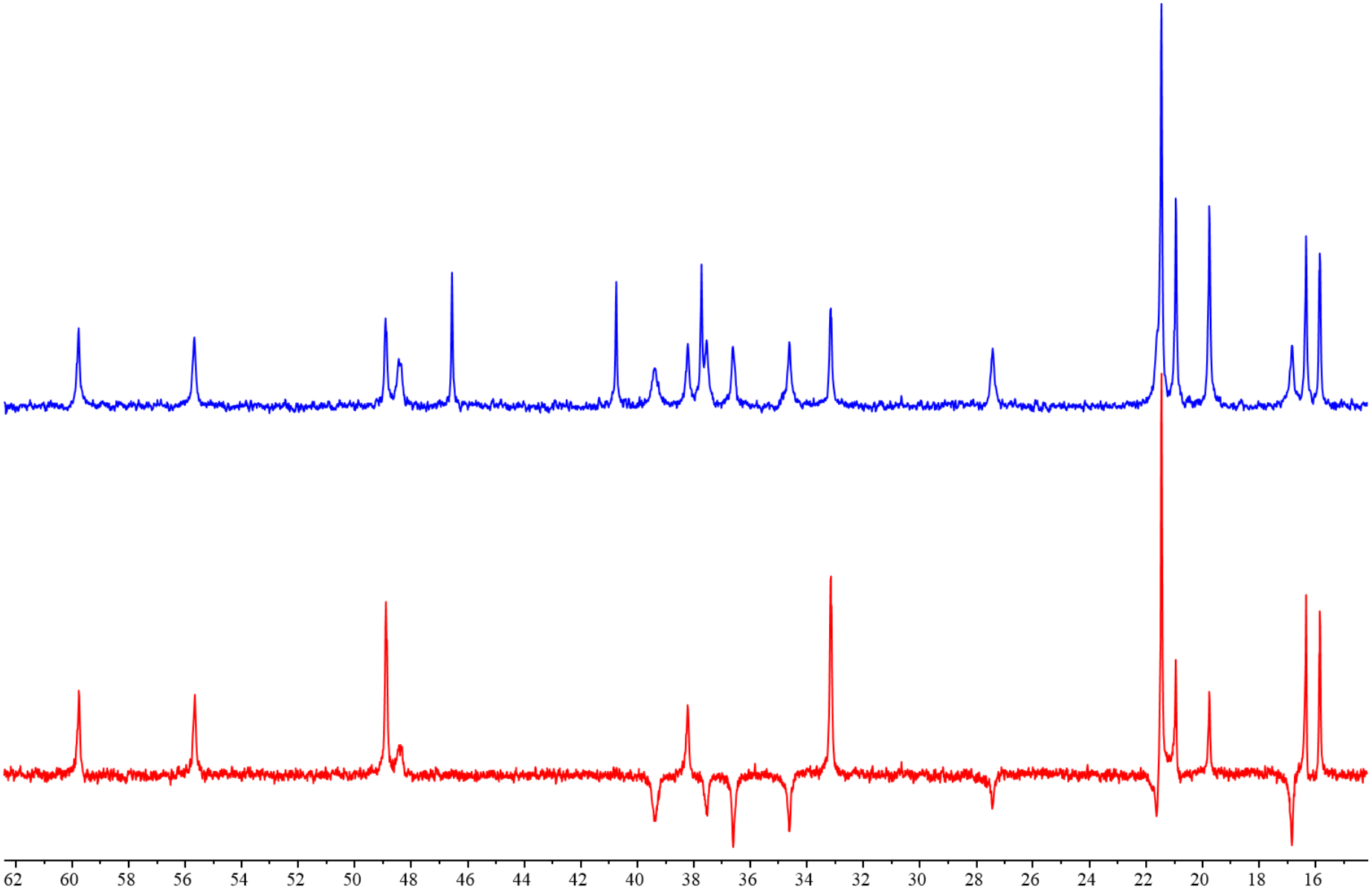

Figure S23. Fragment (δ_C 62-14 ppm) of $^{13}C–\{^1H\}$ and $^{13}C–\{^1H\}$-dept NMR ($CDCl_3$, 101 MHz) spectra of phosphonium salt **2b**.

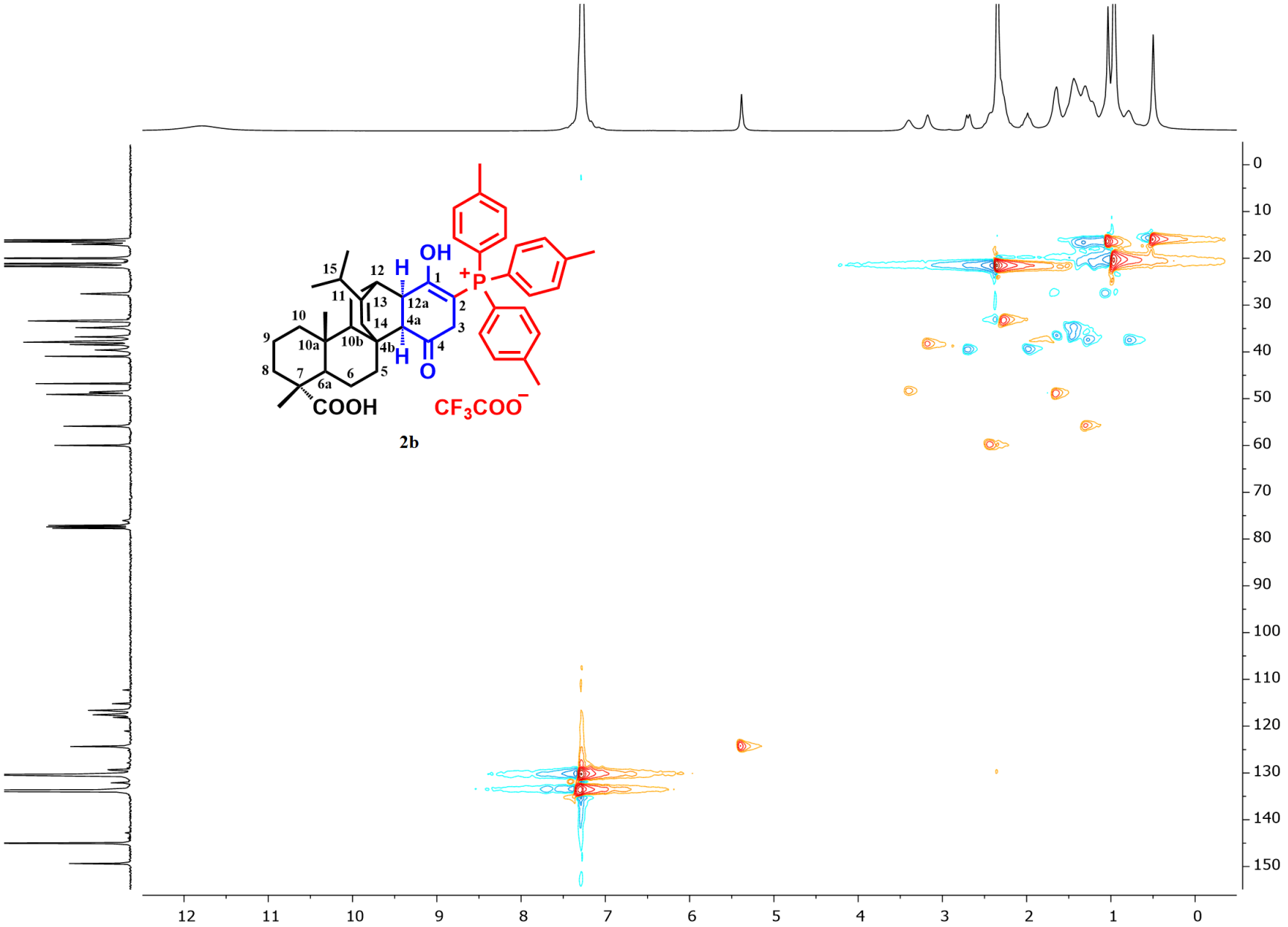

Figure S24. $^{1}H^{13}C$-HSQC NMR ($CDCl_3$, 101 MHz) spectrum of phosphonium salt **2b**.

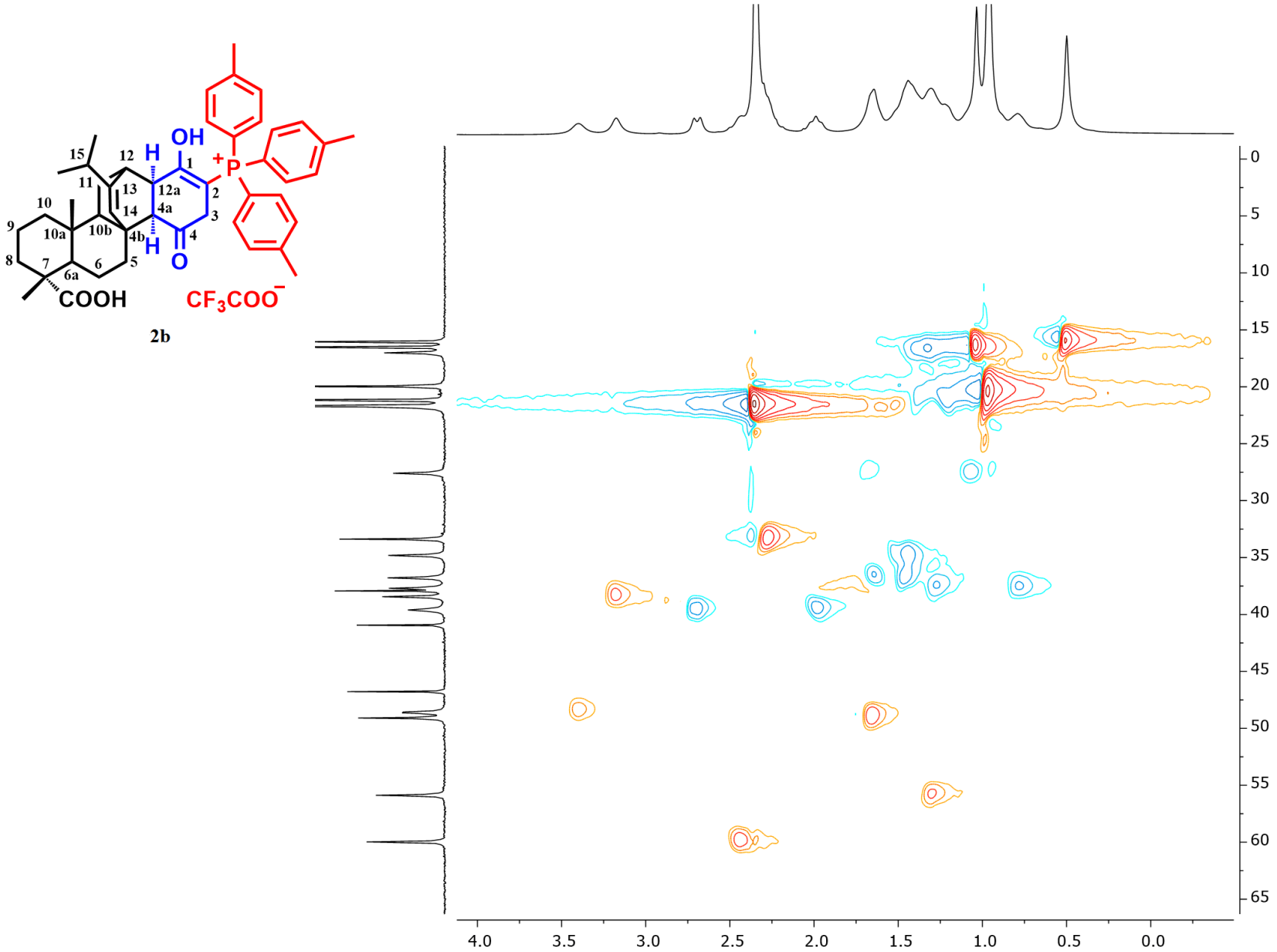

Figure S25. Fragment of $^{1}H^{13}C$-HSQC NMR ($CDCl_3$, 101 MHz) spectrum of phosphonium salt **2b**.

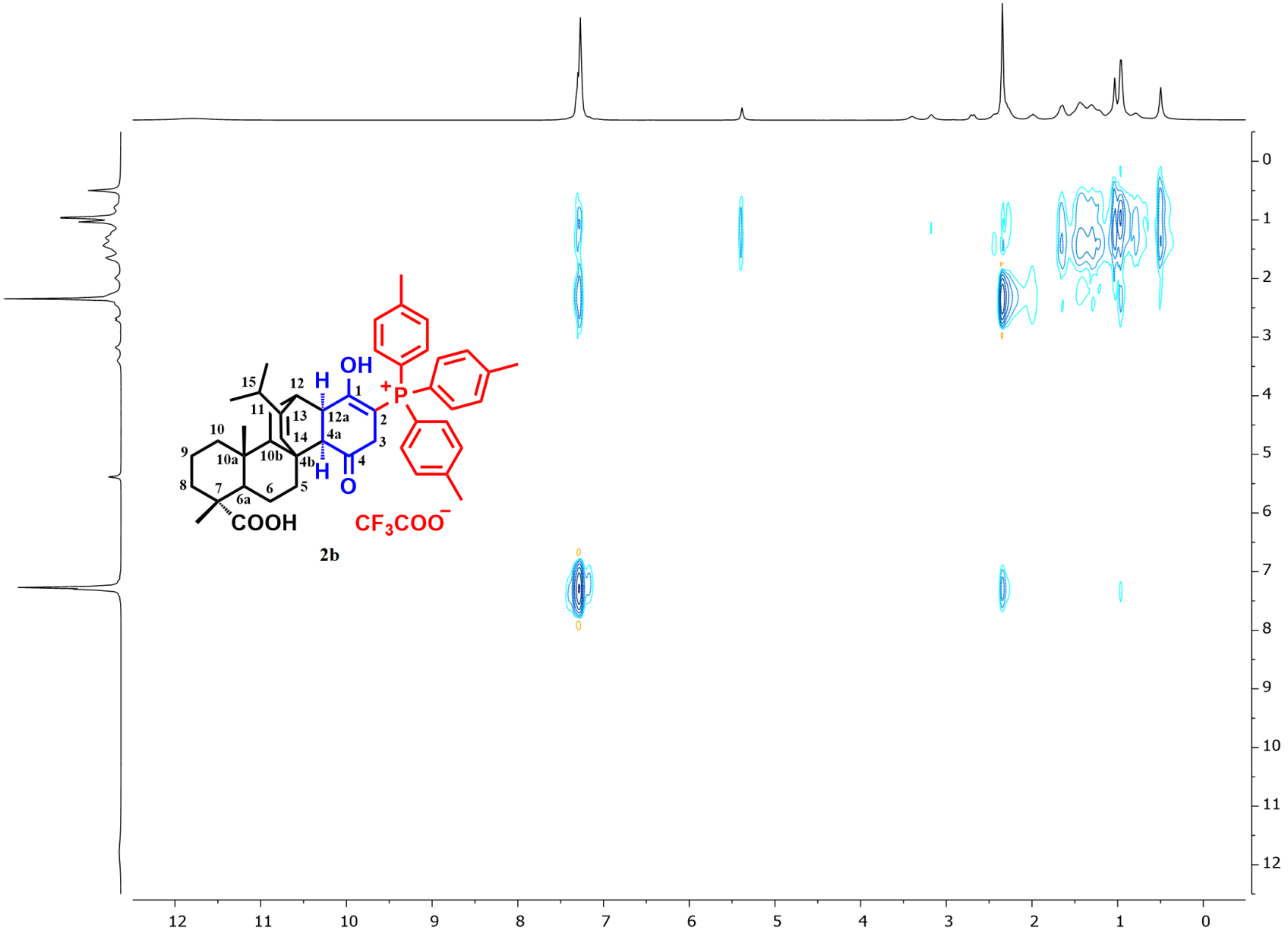

Figure S26. $^{1}H^{1}H$-NOESY NMR ($CDCl_3$, 101 MHz) spectrum of phosphonium salt **2b**.

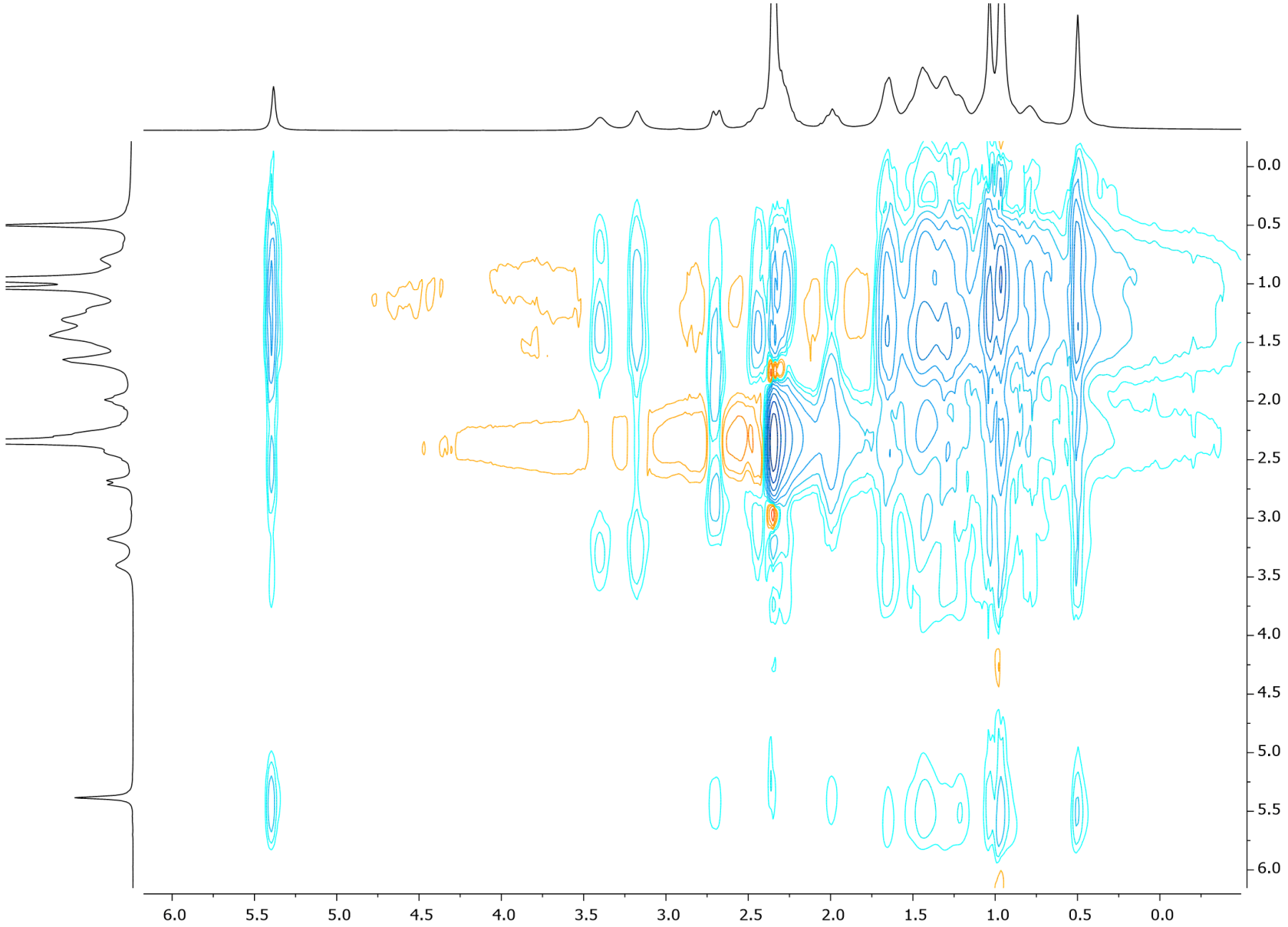

Figure S27. Fragment of $^{1}H^{1}H$-NOESY NMR ($CDCl_3$, 101 MHz) spectrum of phosphonium salt **2b**.

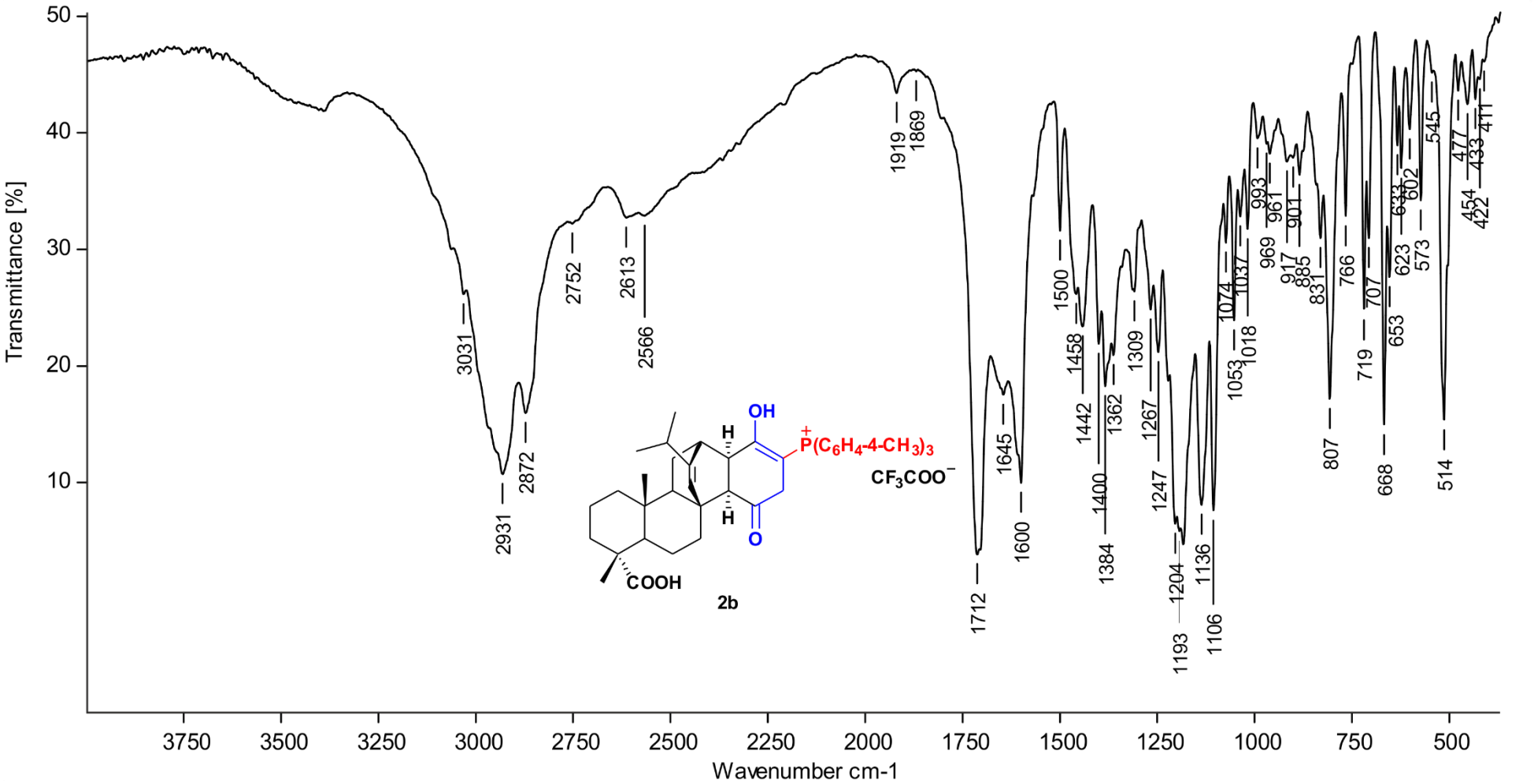

Figure S28. IR (KBr) spectrum of phosphonium salt **2b.**

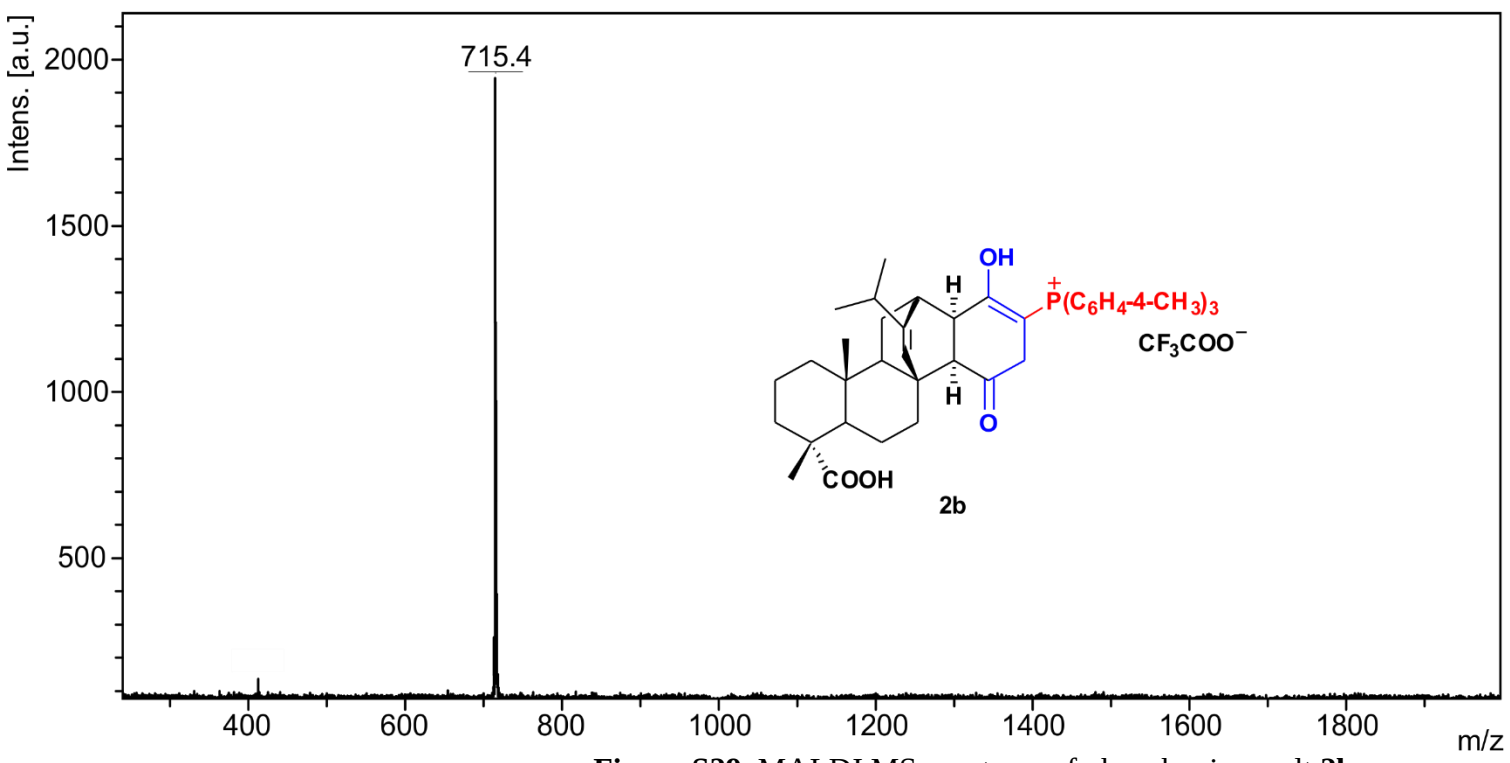

Instrument

Instrument type	ultraflexTOF/TOF
Name of computer	MALDI
flexControl version	flexControl 3.0.173.0
flexAnalysis version	3.0.96.0

Spectrometer

Ion Polarity	POS
PIE delay	50 ns
Ion source voltage 1	20 kV
Ion source voltage 2	19.01 kV
Lens voltage	6 kV
Linear detector voltage	1.498 kV
Reflector voltage 1	0 kV
Reflector voltage 2	0 kV
Reflector detector voltage	1.604 kV

Laser

Ion Source Type	MALDI
Laser Type	Nd:YAG
Wavelength	355 nm
Number of shots	100
Laser repetition rate	100 Hz

Target

Target Plate	MTP AnchorChip
Position	B11

Figure S29. MALDI MS spectrum of phosphonium salt **2b.**

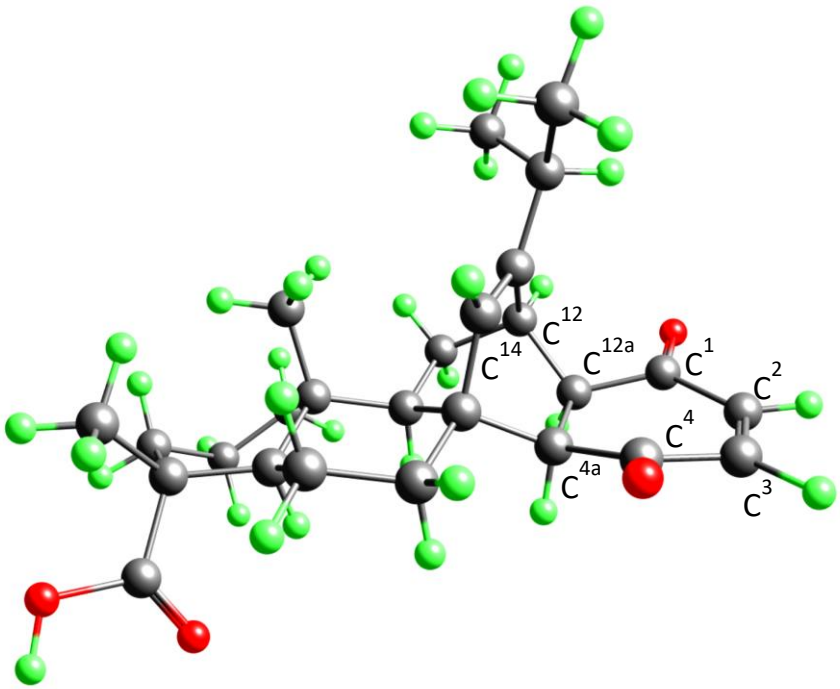

1

selected dihedral angles (°): C(1)–C(2)–C(3)–C(4) –2.0192; O=C(1)–C(2)–C(3) 168.7107; O=C(4)–C(3)–C(2) –156.2662; C(12a)–C(1)–C(2)–C(3) –13.4513; C(4a)–C(4)–C(3)–C(2) 25.9988; C(1)–C(12a)–C(4a)–C(4) 14.2817

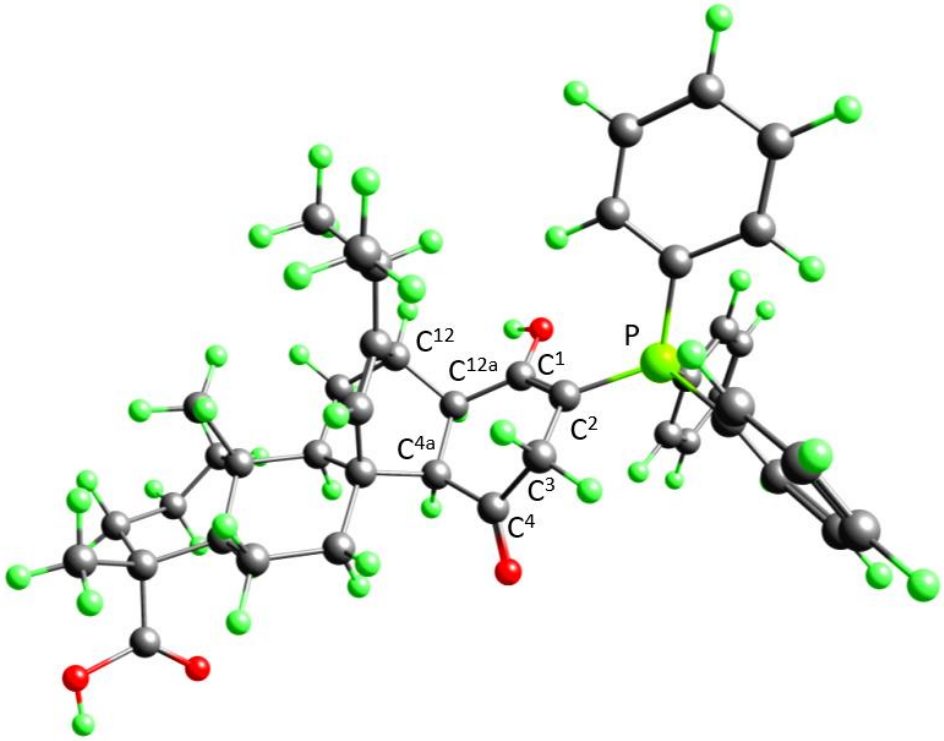

2a

selected dihedral angles (°): C(4a)–C(12a)–C(1)–C(2) 2.7141; O–C(1)–C(2)–P –9.3548; C(4a)–C(4)–C(3)–C(2) –10.3625; C(1)–C(2)–C(3)–C(4) 4.1368; C(1)–C(12a)–C(4a)–C(4) –8.5645; =O–C(4)–C(3)–C(2) 167.0923; C(4)–C(3)–C(2)–P –163.6698

Figure S30. The possible conformers of quinopimaric acid **1** and **2a** according to DFT B3PW91 method.

Table S1. Calculated charges on atoms (NBO analysis) of quinopimaric acid.

Atom number	Charge
C^{1}	0.50817
C^{12a}	–0.30770
C^{2}	–0.22990
C^{3}	–0.21323
C^{4}	0.52053
C^{4a}	–0.30623
$\underline{O}(C^{1})$	–0.50300
$\underline{O}(C^{4})$	–0.49974